



# Probabilistic trajectory generation using uncertainty propagation model

<b>Deliverable ID:</b>	D2.2
<b>Dissemination Level:</b>	PU
<b>Project Acronym:</b>	START
<b>Grant:</b>	893204
<b>Call:</b>	Call: H2020-SESAR-2019-2
<b>Topic:</b>	SESAR-ER4-15-2019-Increased Levels of Automation for the ATM Network
<b>Consortium Coordinator:</b>	[company short name]
<b>Edition date:</b>	28 May 2021
<b>Edition:</b>	00.01.00
<b>Template Edition:</b>	02.00.02

Founding Members



## Authoring & Approval

### Authors of the document

Name/Beneficiary	Position/Title	Date
Andrés Muñoz (BDG)	WP2 leader	25/05/2021
Manuel Polaina (BDG)	WP2 contributor	25/05/2021
Jordi Pons-Prats (UPC)	WP2 Contributor	25/05/2021
Xavier Prats (UPC)	Task 2.1 and 4.1 Leader	25/05/2021

### Reviewers internal to the project

Name/Beneficiary	Position/Title	Date
Manuel Soler (UC3M)	WP1 leader and PC	28/05/2021
Andrés Muñoz (BDG)	WP2 leader	28/05/2021
Emre Koyuncu (ITU)	WP3 leader	28/05/2021
Daniel Delahaye (ENAC)	WP4 leader	28/05/2021
Raimund Zopp (FLIGHTKEYS)	WP5 leader	28/05/2021
Alexander Kuenz (DLR)	WP6 leader	28/05/2021
Xavier Prats (UPC)	Task 2.1 and 4.1 Leader	28/05/2021

### Approved for submission to the SJU By - Representatives of beneficiaries involved in the project

Name/Beneficiary	Position/Title	Date
Manuel Soler (UC3M)	WP1 leader and PC	28/05/2021

### Rejected By - Representatives of beneficiaries involved in the project

Name/Beneficiary	Position/Title	Date
------------------	----------------	------

### Document History

Edition	Date	Status	Author	Justification
00.00.01	04/04/2021	Initial Draft	Andrés Muñoz	New document
00.00.02	25/05/2021	Complete Draft	Andrés Muñoz	Sent for internal review
00.01.00	28/05/2021	Submitted version	Andrés Muñoz	Submission

**Copyright Statement: © – 2021 –START Consortium – All rights reserved. Licensed to the SJU under NO conditions.**

Founding Members



# START

## A STABLE AND RESILIENT ATM BY INTEGRATING ROBUST AIRLINE OPERATIONS INTO THE NETWORK

This Deliverable is part of a project that has received funding from the SESAR Joint Undertaking under grant agreement No 893204 under European Union's Horizon 2020 research and innovation programme.



### Abstract

---

This document establishes the basis for the work to be developed within Work Package 2 of the START project. The objective of this Work Package is to build a methodology that could allow for the obtainment of the probabilistic trajectories that would result from the propagation of the characterized micro-level uncertainties in the aircraft trajectory prediction process. This deliverable will be focused on implementing the models and processes required to capture the influence of the uncertainties that are present in the development of an aircraft trajectory. To this end, we will show how to propagate these uncertainties, using a stochastic trajectory predictor, that will allow us to obtain a set of probabilistic trajectories from an initial deterministic flight plan, which will encapsulate the effect of the inputs' variability.

First, an introduction to Polynomial Chaos Theory, which is the basis of the stochastic trajectory predictor developed in START, and our solution for introducing weather uncertainty into the trajectory prediction process will be exposed. Then, it will be presented how the integration of the advanced data assimilation models, introduced in the deliverable D2.1 [2], together with the stochastic trajectory predictor will lead to more robust airline operations. Additionally, the framework for the probabilistic trajectory generation will be introduced, showing how all different modules will be employed in START in a two-phase approach (first an off-line fitting phase to obtain the models for uncertainty propagation, and then an online phase where, making use of the fitted model, the probabilistic trajectories can be obtained from a deterministic flight plan). Finally, a study case will be presented, showing the application of the previously defined methodology to a specific scenario.



## Table of Contents

Abstract .....	3
<b>1 Introduction.....</b>	<b>7</b>
1.1 START project goals .....	7
1.2 START work plan .....	8
1.3 Purpose and scope of the deliverable .....	9
1.4 Intended readership .....	10
1.5 Acronyms .....	10
<b>2 Modelling aircraft trajectories with uncertainty propagation .....</b>	<b>12</b>
2.1 Introduction .....	12
2.2 Applying arbitrary Polynomial Chaos Theory .....	13
2.3 Considering weather uncertainties.....	16
2.4 Integration of data assimilation models .....	18
<b>3 Probabilistic trajectory generation framework .....</b>	<b>19</b>
3.1 Building the aPCE polynomials .....	19
3.2 Probabilistic trajectory generation .....	30
<b>4 Use case.....</b>	<b>34</b>
4.1 Considering aircraft intent uncertainties .....	34
4.2 Including uncertainty in weather conditions.....	43
4.3 Including uncertainty in initial conditions .....	47
<b>5 Concluding remarks .....</b>	<b>51</b>
<b>6 References.....</b>	<b>52</b>



## List of Tables

Table 1: Acronyms.....	11
Table 2: START consortium acronyms.....	11
Table 3: Values for the calculated collocation points for all LEMD-EDDM trajectories between June 2017 and May 2018.....	36
Table 4: Values for the perturbations introduced to the aircraft intent variables for all flights between LEMD and EDDM during June 2018.....	38

## List of Figures

Figure 1 START project concept schema.....	8
Figure 2 START project work package breakdown.....	9
Figure 3 Structure for the fitting process of the aPCE polynomials.....	20
Figure 4 Structure for the generation of probabilistic trajectories from demand data.....	31
Figure 5 Histograms of values of the considered aircraft intent variables for all optimized LEMD-EDDM trajectories between June 2017 and May 2018. Calibrated airspeeds are provided in knots, pressure altitudes in FL. Solid red lines indicate mean values, dashed red lines indicate the values for the standard deviation. Dashed yellow lines indicate the range of values considered for the calculation of the collocation points.....	35
Figure 6 Probability density function of the difference between planned and observed values for the first block of aircraft intent variables.....	37
Figure 7 Probability density functions of the difference between planned and observed values for the second block of aircraft intent variables.....	37
Figure 8 Histogram for the real flight times for all flights between LEMD and EDDM during June 2018.....	39
Figure 9 Probability density function of the error incurred in the flight time estimation for all flights between LEMD and EDDM during June 2018.....	39
Figure 10 Probability density function of the estimated flight times for all flights between LEMD and EDDM during June 2018 by (top) the trajectory prediction tool and (bottom) the aPCE polynomials	40
Figure 11 Probability density function of the error incurred in the flight time estimation with the reduced set of input variables.....	42



Figure 12 Probability density function of the estimated flight times with the reduced set of input variables for all flights between LEMD and EDDM during June 2018 by a) the trajectory prediction tool and b) the aPCE polynomials..... 43

Figure 13 Results for low-order reconstruction of weather data at three different pressure levels for the POD method. Top row refers to reference data, while bottom one refers to POD low-order reconstructions. Contour plot refers to temperature fluctuations with respect to the mean temperature at each level, while arrows heading and length refer to the direction and intensity of the wind component in the Earth-surface-parallel directions. Arrow colour denotes the magnitude of the wind in the Earth-surface-normal direction. All quantities are scaled with their corresponding standard deviation..... 44

Figure 14 Results for low-order reconstruction of weather data at three different pressure levels for the CNN-AE method. Top row refers to reference data, while bottom one refers to CNN-AE low-order reconstructions. Contour plot refers to temperature fluctuations with respect to the mean temperature at each level, while arrows heading, and length refer to the direction and intensity of the wind component in the Earth-surface-parallel directions. Arrow colour denotes the magnitude of the wind in the Earth-surface-normal direction. All quantities are scaled with their corresponding standard deviation..... 45

Figure 15 Probability density function of the error incurred in the flight time estimation with the aircraft intent set of input variables together with weather variables. .... 46

Figure 16 Probability density function of the estimated flight times with the aircraft intent and weather set of input variables for all flights between LEMD and EDDM during June 2018 by a) the trajectory prediction tool and b) the aPCE polynomials..... 47

Figure 17 Probability density function of the estimated turnaround time for (left) E195 and (right) A320 aircraft operating flights with departure from LEMD to EDDM during June 2018 ..... 49

Figure 18 Probability density function of the estimated taxi times for all flights departing from LEMD during June 2018 for runway (top left) 14L (top right) 14R (bottom left) 36L (bottom right) 36R..... 49



# 1 Introduction

---

## 1.1 START project goals

The development, implementation and validation of optimization algorithms for robust airline operations that result in stable and resilient Air Traffic Management (ATM) performance even in disturbed scenarios is the overall goal of START. To reach this goal, START will combine various methods from applied mathematics, i.e., mathematical optimization, optimization under uncertainty, Artificial Intelligence (AI) and data science, as well as algorithm design. Furthermore, insight into the uncertainties relevant to Trajectory-Based Operations (TBO) systems will be gained through simulations. According to START's Project Management Plan (PMP) [1], the main focus of the project is the optimization of conventional traffic situations while considering disruptive weather events such as thunderstorms.

The main uncertainty sources considered in this project can be classified as:

1. Uncertainties at the micro-level or trajectory level, e.g., due to inaccurate wind forecasts, aircraft performance models, aircraft weight estimation, aircraft intent, and take-off times.
2. Uncertainties at the macro-level or ATM network level, e.g., due to disruptive events in the network such as thunderstorms, congested airspaces or airports, and propagation of micro-level (trajectory level) delays over the network.

Within the main goal stated above, the following specific goals arise:

1. To model uncertainties at the micro (trajectory) level, assimilate air traffic observations every 15 minutes using advanced data science methods, and propagate trajectory uncertainties using assimilated models and a stochastic trajectory predictor.
2. To model uncertainties at the macro (ATM network) level, assimilate observations (satellite data for storm and network status) every 15 minutes using advanced data science methods and propagate ATM network uncertainties using the assimilated models.
3. To develop an AI algorithm capable of generating a set of pan-European (i.e., considering the whole traffic over Europe) robust trajectories that make the European ATM system resilient when facing these relevant uncertainties.
4. To implement those algorithms as an advanced flight dispatching demo functionality for airspace users to obtain robust trajectories.
5. To validate these concepts through system-wide simulation procedures in order to evaluate their stability, assessing the benefits for both the airspace users and the network manager. Recommendations for the derivation of resilient TBO networks will be derived.

The overall concept underpinning the project is sketched in Figure 1. In this structure, one can identify five blocks (each of them corresponding to the five specific goals of the project), namely: Micro-Level (trajectories); Macro-level (ATM Network); AI Metaheuristic Algorithm; Flight dispatching tool; Fast-Time Simulations.

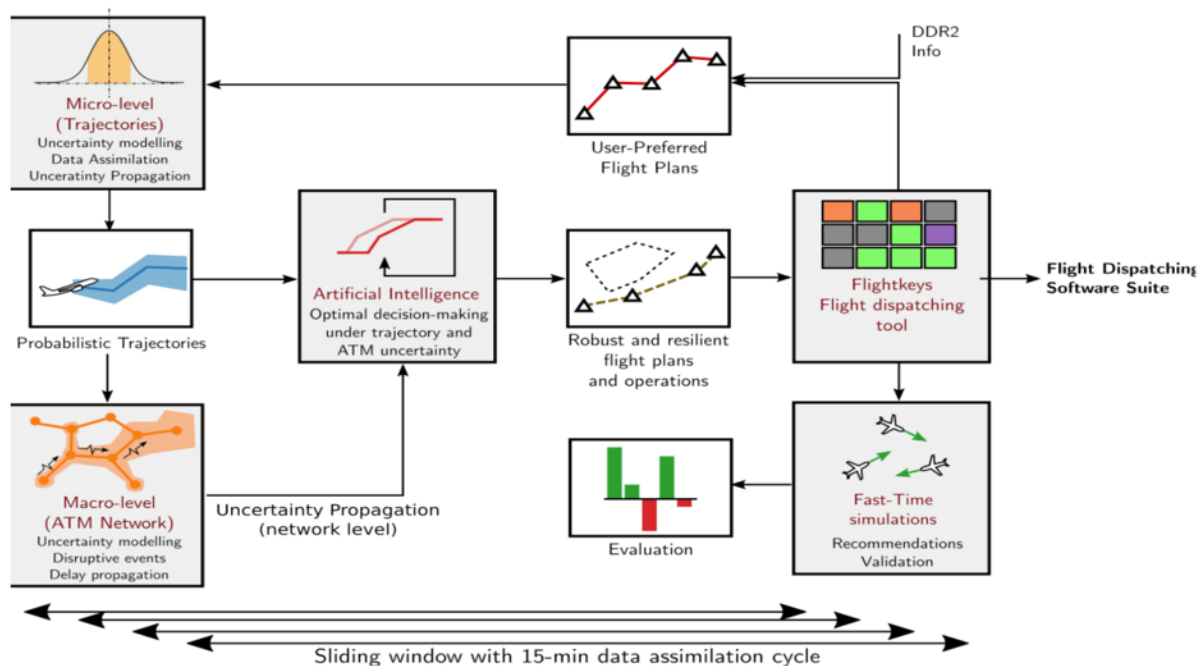


Figure 1 START project concept schema

## 1.2 START work plan

According to START’s PMP [1], the project is divided into seven Work Packages (WP), as sketched in Figure 2, which describes the different tasks to be performed in START. The objectives of each WP are the following:

- WP1 - Project management: The goal is to effectively fulfil all the administrative, contractual, financial and technical aspects of the coordination of the project.
- WP2 - Trajectory level - Uncertainty modelling, data assimilation and uncertainty propagation: The goal is to develop uncertainty propagation models at trajectory level; identify and characterize potential sources of trajectory level uncertainty following a data-driven approach; build and develop methods for the cyclic ingestion of data inputs that will feed the uncertainty propagation models at the trajectory level.
- WP3 - ATM network level - network modelling, uncertainty propagation with disruptive events: The goal is to develop an approximate ATM network model from the historical data enabling to simulate and analyse uncertainty and delay propagation; integrate individual trajectory uncertainties into the network model; provide models for disruptive events and integrate them into the network-wide model; validate the model, procedures and provide a simulation environment/tool for use case analyses.
- WP4 - Network-wide robust trajectory planning and resiliency management based on simulating annealing: The goal is to formulate a concept of operations implementing TBO allowing for the appropriate management of uncertainty; formulate the network resiliency and develop network resiliency management procedures in case of disruptive events; develop optimization algorithms for the determination of efficient strategic interventions that increase



the predictability and resiliency of ATM operations and validate the proposed methods through use case simulation and analysis.

- WP5 - Flight dispatching prototype tool: The goal is to validate the concept in a simulated dispatch environment of one or more airline operators, utilizing the FLIGHTKEYS5D flight management system.
- WP6 - Simulation and validation: The goal is to validate the concept in a simulated dispatch environment of one or more airline operators, utilizing the FLIGHTKEYS5D flight management system.
- WP7 Dissemination, exploitation and communication: The goal is to coordinate all START dissemination, exploitation, and communication activities while ensuring that the different targets have been reached.

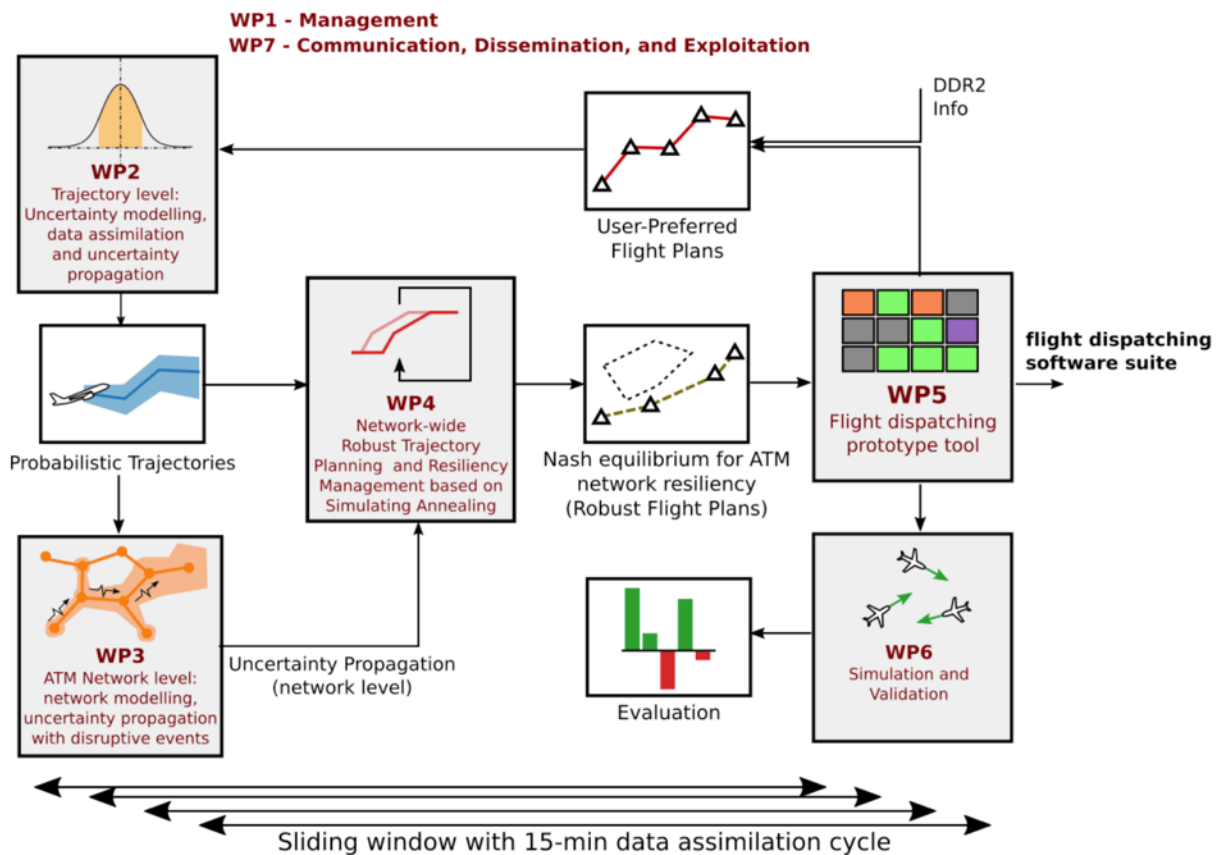


Figure 2 START project work package breakdown

### 1.3 Purpose and scope of the deliverable

START proposes a framework for obtaining robust airline operations that lead to a stable and resilient ATM performance in any kind of disruptive scenario by means of a combination of methods from applied mathematics. Consequently, the focus will be on providing the capabilities required to update the planned flight trajectories according to the uncertainties introduced by the disturbances in the considered air traffic scenarios, which would be a key enabler for the implementation of the TBO

concept. For this purpose, introducing the capability of identifying potential disturbances in the system and optimizing the air traffic operations to adapt to their associated uncertainty at different operational levels, was considered an essential feature of the framework.

With regards to this main focus of START, Work Package 2 will address all the technical challenges related to three main tasks:

- Identify and characterize the sources of uncertainty that may affect the evolution of the trajectory and that stem from the micro or trajectory level.
- Model how these uncertain factors influence the development of the planned trajectory.
- Ingest data on a continuous fashion that provides an input on the status of the uncertainty sources in the pre-tactical phase of the considered air traffic scenario.

After the identification and characterization of micro-level uncertainties and the implementation of advanced data assimilation models explained in the deliverable D2.1 [2], this deliverable describes the methodology followed to propagate uncertainties at trajectory level. For this purpose, the formulation and implementation of the Polynomial Chaos (PC) theory and a weather dimensionality reduction framework will be presented in order to obtain a stochastic trajectory predictor.

Furthermore, the integration of the different modules and models introduced in D2.1 will be explained, as well as how the system obtained from this integration can be employed to obtain a set of probabilistic trajectories from an initial input flight plan. To assess the validity of the proposed methodology, a study case using real data will also be presented in the final section of this deliverable.

## 1.4 Intended readership

This document is intended to be used by START members and SJU (included the Commission Services).

## 1.5 Acronyms

Non-exhaustive list of acronyms used across the text.

Acronym	Description
aPCE	Arbitrary Polynomial Chaos Expansion
ADS-B	Automatic Dependent Surveillance Broadcast
AI	Artificial Intelligence
ATM	Air Traffic Management
ATS	Air Traffic Service
CAS	Calibrated Airspeed
CI	Cost Index
CNN-AE	Convolutional Neural Networks – Auto Encoder
DDR2	Demand Data Repository
ECMWF	European Center for Medium-Range Weather Forecasts
EPS	Ensemble Prediction System

FPO	Flight Plan Optimization
FRA	Free Route Areas
ILS	Instrumental Landing System
METAR	Meteorological Aerodrome Reports
NOAA	National Oceanic and Atmospheric Administration
PC	Polynomial Chaos
PMP	Project Management Plan
POD	Proper Orthogonal Decomposition
ROC	Rate of Climb
TBO	Trajectory-Based Operations
TOC	Top of Climb
TOD	Top of Descent
TP	Trajectory Prediction
WP	Work Package

**Table 1: Acronyms**

START Consortium

Acronym	Description
BDG	Boeing Research and Technology Europe-Germany
DLR	German Aerospace Center
ENAC	École Nationale de l'Aviation Civile
FLIGHTKEYS	FlightKeys
ITU	Istanbul Teknik Universitesi
UC3M	Universidad Carlos III de Madrid
UPC	Universitat Politecnica de Catalunya

**Table 2: START consortium acronyms**

## 2 Modelling aircraft trajectories with uncertainty propagation

---

### 2.1 Introduction

The determination of the influence of micro-level uncertainties in the evolution of a planned aircraft trajectory is the core problem to be tackled in this section of the START project. Quantifying and modelling the effect of these uncertain factors when issuing the prediction for the aircraft trajectories to be considered in any potential air traffic scenario is a key step in the development of the capabilities for proposing robust and resilient airline operations.

The identification of the uncertain factors that affect the aircraft trajectory prediction process was well covered in deliverable D2.1 [2], as well as its characterization using a data-driven approach that relies on historical data instances coming from various information sources. Therefore, this deliverable refers to this previous document for the necessary activities to be executed prior to the complex task of incorporating these quantified uncertainties to the trajectory prediction activities, which will be developed in this document.

Starting our analysis from the conclusions extracted in [2], it will be paramount to develop the capabilities to assess the impact of the variability of the identified stochastic factors on the trajectory predictions to be calculated. It was seen that the actual values to be adopted by the inputs affecting the prediction process (aircraft intent, initial state, aircraft performance and weather conditions) are uncertain, and will most probably vary with respect to the nominal values available for the prediction (e.g., declared flight plan, weather forecasts).

Deviations are then expected and observed between the predicted and actual trajectories, which can be considered as an error associated to the deterministic prediction of the aircraft trajectory due to the stochastic variability of the considered inputs (sensitivity of the aircraft trajectory prediction process to the variability of the inputs is well studied [3][4]). As such, it is essential to assess how said variability affects the output predicted trajectories to be obtained, as the spectrum of possible predictions will depend on the value distributions for each of the identified uncertain input variables. These distributions were characterized in [2] for the proposed uncertain factors, so now the focus is on determining how to propagate these uncertainties along the aircraft trajectory prediction process, so that an assessment can be obtained on the effect of the inputs' variability on the predicted trajectory from a nominal flight plan.

This is a problem that has been tackled in previous instances that can be found in the literature. The classical methodology applied to uncertainty propagation problems in dynamic systems normally relies on Monte Carlo simulations to evaluate the variability of inputs on the output trajectories by applying statistical methods to the numerous simulated runs. Examples of these are available with different methodologies to model the variability of a different range of uncertain inputs, such as neural networks for single trajectory variables in various flight phases [5] or cause-effect models for interdependent uncertainties [6], or including worst-case prediction algorithms [7]. Although the application of Monte Carlo simulations seems simple and straightforward in these problems, it has a clear limitation on scalability for large air traffic scenarios, as it is very computationally demanding and

time consuming. These limitations were also acknowledged on similar studies regarding aircraft trajectory predictions [8][9].

An alternative method with respect to Monte Carlo approaches that provides an increased computational efficiency while establishing a framework for uncertainty propagation is based on the Polynomial Chaos theory. This fact has been stated widely and its benefits shown in previous literature work, as for example in a similar problem tackled in the COPTRA project [10] or in [11], as well as in specific studies regarding the sensitivity of the arrival time output taking into account aircraft intent uncertainty [12] or the propagation of mass uncertainty for cruise phases [13].

Therefore, the implementation of the PC theory will be selected for the propagation of the identified and quantified sources of uncertainty along the trajectory prediction process. This will be done in order to obtain an assessment on the potential probabilistic trajectories that can be output for an initial flight plan as a function of the spectrum of values to be adopted by the characterized uncertain inputs for the aircraft trajectory prediction process. The formulation and implementation of the PC theory, along with the integration of additional modules to support the process, will be developed in the following sections.

## 2.2 Applying arbitrary Polynomial Chaos Theory

### 2.2.1 Theoretical framework

Chaos theory, introduced by Norbert Wiener in 1938 [14], proposes that any function or model  $z$  dependent of a stochastic variable  $\xi$  can be posed as a linear combination of coefficients  $a_i(t)$ , independent of the stochastic variable, times a set of one-dimensional polynomials  $\gamma_i(\xi)$ , which form a basis orthogonal to the probabilistic distribution of the stochastic variable  $\xi$ , such that:

$$z(t, \xi) = \sum_{i=1}^{\infty} a_i(t) \gamma_i(\xi) \approx \sum_{i=1}^d a_i(t) \gamma_i(\xi) \quad (1)$$

Where the subindex  $i$  refers to polynomial degree. Whereas the approximation error disappears when  $i$  tends to infinity, it is common practice to truncate the model at certain polynomial degree  $d$ . Nonetheless, any realistic model representing a physical mechanism depends on several stochastic parameters such that  $\xi = \{\xi_1, \xi_2, \xi_3, \dots, \xi_N\}$ . Henceforth, the total number of stochastic input parameters will be referred as  $N$ . Consequently, Equation (1) needs to be reformulated as a multidimensional polynomial expansion as follows:

$$z(t, \xi_1, \xi_2, \dots, \xi_N) = \sum_{i=1}^{\infty} b_i(t) \Gamma_i(\xi_1, \xi_2, \dots, \xi_N) \quad (2)$$

Where  $b_i(t)$  still quantifies the model's dependence on the polynomial expansion, while  $\Gamma_i(\xi_1, \xi_2, \dots, \xi_N)$  contains a multidimensional orthogonal polynomial basis for the stochastic variables  $\xi$ . Assuming that the stochastic input variables  $\xi$  are independent of each other, the multidimensional basis can be constructed as a simple product of the one-dimensional polynomials, such that:

$$\Gamma_i(\xi_1, \xi_2, \dots, \xi_N) = \prod_{j=1}^N \gamma_j^{\alpha_j^i}(\xi_j) \quad (3)$$

Where the index  $\alpha_j^i$  is used to indicate the combinatoric information between the different independent variables and the polynomial degrees.

$$\sum_{j=1}^N \alpha_j^i \leq M, \quad i = 1, \dots, N \quad (4)$$

The number  $M$  of possible combinations between the different stochastic variables and polynomials degrees is defined as:

$$M = \frac{(N + d)!}{N! d!} \quad (5)$$

Thus, allowing to picture  $\alpha_j^i$  as  $M \times N$  matrix containing the corresponding degree of the stochastic variables for each combination.

## 2.2.2 Definition of aPCE polynomial expansions

While there are several methods to compute these polynomials based on predefined probability density functions such as normal, gamma, beta or uniform, this project tackles these polynomials construction from a data-driven point of view, for which the arbitrary Polynomial Chaos Expansion (aPCE) [15] method is used. This method uses the statistical moments for each stochastic variable, calculated as:

$$\mu_k = \int \xi_i^k dP(\xi_i) \quad (6)$$

With this method, each polynomial  $\gamma_i^k$  is defined with a set of polynomial coefficients  $c_m^{(k)}$  multiplied by their corresponding power of the stochastic variable  $\xi_i$

$$\gamma_i^k = \sum_{m=0}^k c_m^{(k)} \xi_i^m \quad (7)$$

$$c_{m=k}^{(k)} = 1 \quad (8)$$

For each stochastic variable, the polynomial coefficients can be computed by ensuring the orthogonality between two polynomials of order  $k$  and  $l$  such that:

$$\int \gamma^k \cdot \gamma^l \cdot dP(\xi_i) = \delta_{k,l} \quad (9)$$

Where  $\delta_{k,l}$  is the Kronecker delta and is equal to 0 unless  $k$  is equal to  $l$ . Subsequently, a set of equations can be defined for each polynomial degree such that:

$$\int c_0^{(0)} \cdot \left[ \sum_{m=0}^l c_m^{(k)} \xi_i^m \right] \cdot dP(\xi_i) = 0 \quad (10)$$

$$\int \left[ \sum_{m=0}^1 c_m^{(1)} \xi_i^m \right] \cdot \left[ \sum_{m=0}^l c_m^{(k)} \xi_i^m \right] \cdot dP(\xi_i) = 0 \quad (11)$$

$$\vdots$$

$$\int \left[ \sum_{m=0}^{k-1} c_m^{(k-1)} \xi_i^m \right] \cdot \left[ \sum_{m=0}^l c_m^{(k)} \xi_i^m \right] \cdot dP(\xi_i) = 0 \quad (12)$$

$$\int \left[ \sum_{m=0}^k c_m^{(k)} \xi_i^m \right] \cdot \left[ \sum_{m=0}^l c_m^{(k)} \xi_i^m \right] \cdot dP(\xi_i) = c_m^k = 1 \quad (13)$$

Substituting Equation (6) into Equations (10)-(13) leads to a system of linear equations that can be written in a matrix form.

$$\begin{bmatrix} \mu_0 & \mu_1 & \dots & \mu_k \\ \mu_1 & \mu_2 & \dots & \mu_{k+1} \\ \vdots & \vdots & \ddots & \vdots \\ \mu_{k-1} & \mu_k & \dots & \mu_{2k-1} \\ 0 & 0 & \dots & 1 \end{bmatrix} \begin{bmatrix} c_0^{(k)} \\ c_1^{(k)} \\ \vdots \\ c_{k-1}^{(k)} \\ c_k^{(k)} \end{bmatrix} = \begin{bmatrix} 0 \\ 0 \\ \vdots \\ 0 \\ 1 \end{bmatrix} \quad (14)$$

### 2.2.3 Calculation of the aPCE coefficients

To compute the aPCE coefficients  $b_i(t)$ , the aPCE polynomials  $\gamma_i^k(\xi)$  need to be evaluated at certain points of the stochastic-variable parametric space in order to solve the system of equations defined in Equation (14), where the number of unknowns is defined by Equation (5). Several methods can be found in the literature for this task, such as Galerkin projection [16] or collocation [17] methods, of which we will use the latter.

The collocation method evaluates each polynomial expansion at certain values, known as collocation points, which are extracted from the roots of the next higher-order polynomial for each stochastic parameter [18]. This implies that, for a polynomial of order  $d$ , the number of available collocation points is  $(d + 1)^N$ , which is always larger than the number of unknowns in the system of equations. This overdetermined system is solved by selecting the optimal  $M$  combination of collocation points based on the probability of each combination of collocation points. This probability is computed from the sum of the polynomial degree of each stochastic variable in every combination, assuming that in a standard Gaussian random variable with zero mean and unit variance the higher the root degree the lower the probability to occur.

Each of the  $M$  combinations of collocation points require to compute a solution of  $z(t, \xi_1, \xi_2, \dots, \xi_N)$ . Following [19], the coefficients  $b_i(t)$  can be computed either using Galerkin projection:

$$\left\langle \sum_{k=0}^d b_k \Gamma_k(\xi^{(i)}), \Gamma_l(\xi^{(i)}) \right\rangle = 0 \quad (15)$$

Or least-square approximation:

$$\hat{b}_i(t) = \underset{b}{\operatorname{argmin}} \sum_{i=1}^M \left( z^{(i)} - \sum_{k=0}^d b_k \Gamma_k(\xi^{(i)}) \right) \quad (16)$$

## 2.3 Considering weather uncertainties

As introduced in Section 2.2, the computational cost of arbitrary polynomial chaos expansion increases factorially with the increase of the polynomial degree and the number of variables, as stated in Equation (5). This poses a problem when dealing with systems affected by a large number of stochastic input variables. One of these systems is the effect of weather on the aircraft trajectory as shown in [20], where a robust aircraft trajectory planning tool was presented to account the effects of wind uncertainty. The weather information used for this type of tools is usually stored in large four-dimensional tensors, with three spatial dimensions and one dimension for the relevant quantities describing the atmosphere state. Moreover, the spatial resolution required for aircraft trajectory predictors is normally of the order of  $\mathcal{O}(10^0)$  degree in the longitudinal and latitude direction, while in the altitude direction is discretized in steps of 100 mbar. Taking this into account, a four-dimensional (4D) weather information tensor for Europe may contain a number of variables of the order of  $\mathcal{O}(10^4)$ , which would require  $\mathcal{O}(10^{12})$  collocation points, which is far beyond the scope of computational cost reduction intended for aPCE and the computational capabilities available in the consortium.

To overcome this issue, a dimensionality reduction of the weather information can be carried out, allowing the aPCE to deal with a reduced version of weather. Later, the collocation points provided by aPCE for this reduced-state weather information can be translated back into the original weather dimension, allowing any aircraft trajectory predictor tool to ingest this artificial information. It is important to remark that, although the weather information produced by the aPCE may not have existed before, the techniques used are aimed at maintaining a physical sense. Two different algorithms are used for this dimensionality reduction task, one exploiting the linear relationship of the weather data and the other taking advantage of the modern artificial intelligence techniques designed for this type of tasks.

### 2.3.1 Proper orthogonal decomposition

The first methodology used to reduce the dimensional state of the weather data is the proper orthogonal decomposition (POD), also known as principal component analysis or Karhunen–Loève decomposition. This decomposition states that any function dependent of time  $t$  and space  $x$  can be decomposed in a time-averaged value plus a fluctuating component defined as a linear combination of a spatial basis, composed of spatially orthonormal functions  $\phi_i(x)$ , times a temporal orthonormal basis made of orthonormal function  $\psi_i(t)$ :



$$c(x, t) \approx \bar{c}(x) + \sum_{i=1}^{N_m} \psi_i(t) \sigma_i \phi_i(x) \quad (17)$$

Where the  $N_m$  is the number of orthonormal modes used for the reconstruction.

The practical implementation of POD follows the method of snapshots proposed in [21]. Each weather sample is reshaped in a vector of size  $N_p$ , where this value refers to the total number of variables in each sample. The total number of samples  $N_t$  in vector form are rearranged in a matrix:

$$C = \begin{bmatrix} c(x_1, t_1) & \dots & c(x_{N_p}, t_1) \\ \vdots & \ddots & \vdots \\ c(x_1, t_{N_s}) & \dots & c(x_{N_p}, t_{N_s}) \end{bmatrix} \quad (18)$$

Of size  $N_t \times N_p$ , where each row refers to a sample and each column to a variable.

The matrix  $\Psi$  containing the POD temporal modes can be obtained solving the eigenvalue problem of the temporal correlation matrix  $S$  as follows:

$$S = CC^T = \Psi\Lambda\Psi^T \quad (19)$$

Where  $\Lambda$  is a diagonal matrix with elements  $\lambda_i = \sigma_i^2$  representing the variance content of each mode. The  $\sigma_i$  coefficient can be rearranged in a diagonal matrix  $\Sigma$ . Finally, the matrix  $\Phi$  containing the spatial modes can be obtained by projecting the weather matrix of the temporal basis as:

$$\Phi = \Sigma^{-1}\Psi^T C = \Sigma^{-1}\Psi^T \Psi \Sigma \Phi = \Phi \quad (20)$$

Assuming statistical convergence of the weather dataset used to compute the POD modes, any weather sample (inside and outside of the training dataset) can be quite accurately described as a linear combination of the modes contained in the  $\Sigma\Phi$  matrix by the corresponding time coefficients. Thus, a reduced version of any weather sample can be obtained by truncating the number of POD modes used in the reconstruction and requiring only the temporal coefficients to be embedded on the aPCE as inputs.

### 2.3.2 Convolutional neural network autoencoder

The second methodology is based on autoencoders [22], a type of neural networks that maps a given input  $c$  into a latent space  $q$  using an encoding function  $\mathcal{F}_{enc}(c, w_{enc})$ , and then maps back the latent space into the original input by means of a decoding function  $\mathcal{F}_{dec}(q, w_{dec})$ . Subsequently, any input can be described as:

$$\tilde{c} = \mathcal{F}_{dec}(q, w_{dec}) = \mathcal{F}_{dec}(\mathcal{F}_{enc}(c, w_{enc}), w_{dec}) \quad (21)$$

Where  $w_{enc}$  and  $w_{dec}$  refers to the weight of the encoding and decoding functions respectively. These weights can be fitted using a stochastic gradient descent approach, commonly used in deep learning, to minimize the  $L_2$  norm between the original and reconstructed samples

$$w = \{w_{enc}, w_{dec}\} = \underset{w}{\operatorname{argmin}} \| \tilde{c} - c \|_2^2 \quad (22)$$

It is worth to mention the intrinsic relationship between the POD and autoencoders, since it has been proved that a neural network with a single hidden layer and linear activation function is equivalent to

POD [23]. The nonlinearities inherent to neural networks allow autoencoders to retain more information than POD for the same number of latent-space variables.

Since weather information is characterized by the local spatial dependency of the data, the layers of the autoencoder are built using convolutional neural networks, henceforth referred to as CNN-AE. This type of network allows to exploit the spatial relationship of the data and to reduce the computational cost with respect to a classical autoencoder [24]. The weather information can be compressed into a latent representation to be fed into the aPCE, and the collocation points extracted from this can be translated to the dimensional space of the weather data, in a similar way as in POD approach. One of the benefits of CNN-AE with respect to POD is that the latter is limited by the linearity of the orthonormal basis, while the former can include nonlinearities that allow to capture better the weather information. The CNN-AE nonlinearities are embedded using nonlinear activation functions such as hyperbolic tangent or rectified linear unit [25]. With respect to the stochastic gradient descent approach for the weights fitting, the Adam [26] algorithm has been used.

## 2.4 Integration of data assimilation models

Data assimilation models were introduced in [2] as complementary modules capable of providing an estimation on some of the identified uncertain variables in the trajectory prediction process based on the captured status information of the air traffic system of interest. As such, considering an approximated value for these uncertain parameters avoids the need of modelling their uncertainty using the aPCE process, and offers the possibility of taking into account an approximate value that may be better adapted to the current and updated air traffic situation to be considered.

The integration of these data assimilation models will be focused on calculating an estimate of the initial time of the flight, a parameter that was identified as uncertain for any given flight and that affects the results to be provided by the aircraft trajectory prediction process. As it was documented in Section 2.3 with the weather data, the aPCE process benefits of considering a reduced number of uncertain variables in the calculations. Therefore, considering a data-driven estimation of the initial time allows to remove this uncertain parameter from the aPCE calculation. On top of that, using these data assimilation models for the initial flight time estimation provides the added benefit of taking into account the current status of the system, helping to make the solution to be provided more robust by considering tactical factors.

The proposed data assimilation models will therefore be integrated as an external module to the aPCE calculation process, as they do not need to be embedded within the uncertainty quantification process to be defined for the uncertain variables for which no data assimilation model is built. This can be done for any uncertain parameter that affects the aircraft trajectory for which it would be possible to gather relevant real-time information about and for which the uncertainty characterization is not suitable due to the lack of reference data from the flight plan data. As it was developed in [2], this is true for the initial time of the flight, as the flight plan does not give an exact value for the take-off time and it is possible to retrieve estimations for it, but could be extended to other stochastic variables affecting the trajectory prediction process that are not considered within this work, such as the initial 3D position of the flight.

Estimations provided by the data assimilation models will entail an associated uncertainty due to the potential error to be introduced by the prediction process. Therefore, the estimations to be considered for the uncertain variables to be modelled will consist of a distribution of possible values according to the issued prediction and its associated prediction error.

## 3 Probabilistic trajectory generation framework

---

In this section, the specific implementation of the PC theory for the generation of the probabilistic trajectories needed for later stages of the START project will be detailed. The developed framework is a two-phase system which depends on several inputs coming from different data sources, as well as on multiple standalone modules or tools that have their own inherent complexity. Therefore, the process followed to document the system will go phase by phase and module by module to explain all the developed capabilities throughout the process.

A relevant feature of the developed methodology, as previously mentioned, is that it consists of two separate but sequential phases or structures. The first phase is dedicated to the obtainment of the full definition of the polynomials, posed following the PC theory, that will describe the evolution of the variables characterizing an aircraft trajectory as a function of the time elapsed and of the values adopted by the identified uncertain input variables. This first structure is therefore focused on following a data-driven approach for retrieving the set of polynomial coefficients that are best suited to describe the trajectories of interest, which will have a certain set of common characteristics (e.g., for a specific city pair, for a specific aircraft type, or for both a specific city pair and aircraft type). Parallel to this process, the employed datasets will be leveraged to execute the uncertainty quantification of the identified uncertain variables following the methodology explained in [2], so it is included in this first structure of the system. The whole process for this first phase will be described in Section 3.1

Once the full definition of the polynomials is obtained, the second phase of the system is applied to use them to retrieve the set of probabilistic trajectories that can be associated to a nominal flight plan. This second phase is then dedicated to perturbing an initial flight plan coming from network demand data with the characterized value distributions for the uncertain variables that determine the trajectory evolution as per the PC formulation. This set of perturbations is then fed to the defined polynomials to obtain different trajectories that can be formulated for the input flight plan according to the considered uncertainty spectrum. In this structure, the data assimilation models introduced in [2] will enter the process by providing updates of expected values for some of the uncertain input variables, providing a better assessment of the probabilistic trajectories by reducing the uncertainty associated to the input variables. This second phase of the system will be fully developed in Section 3.2.

### 3.1 Building the aPCE polynomials

This first phase of the framework, as explained before, is focused on obtaining the polynomials that will characterize the evolution of the variables defining the aircraft trajectory. To that end, different modules have to be coordinated in order to have an appropriate trajectory characterization based on a thorough and complex aircraft trajectory prediction process, which will be the base from which the polynomials to be retrieved will be fit. For this purpose, the input datasets to this first phase are the network demand data for the defined past instances, composed of flight plan, surveillance and performance data, as well as the weather information for the established timeframe.

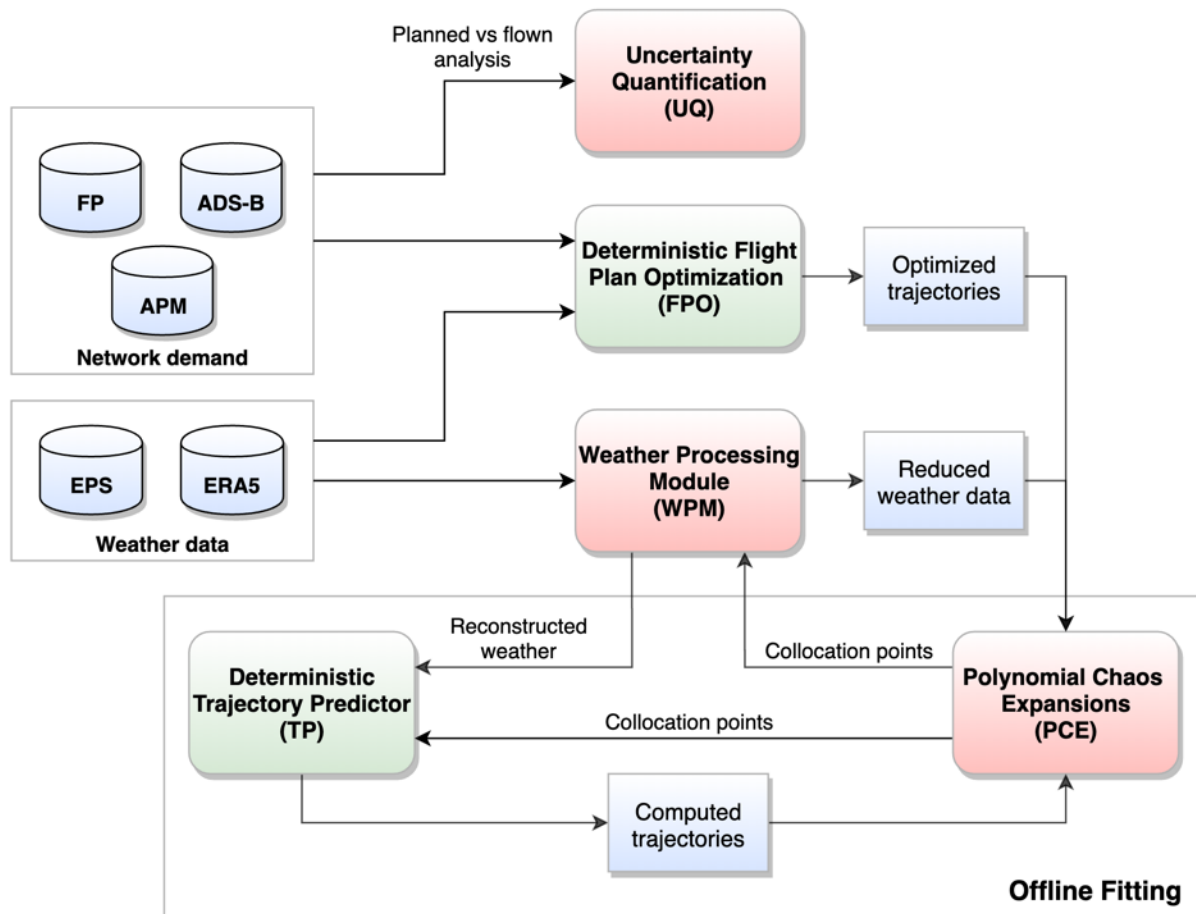


Figure 3 Structure for the fitting process of the aPCE polynomials

The schema showing the process to be followed during this first phase in order to build the aPCE is shown in Figure 3. In this schema, it can be observed that the main structure revolves around the obtainment of the boxes coloured in red, which constitute the modules that will be required in the second phase in order to calculate the established values for the probabilistic trajectories. These three modules are: the polynomials that will allow to describe the aircraft trajectory variables as a function of the possible values of the defined uncertain input parameters, through a fitting process described in Section 3.1.5; the module for integrating the retrieved weather information in order to consider the weather conditions as a potential source for uncertainty affecting the trajectory, described in Section 3.1.6; and the uncertainty quantification process for the uncertain trajectory variables, detailed in Section 3.1.7.

Additional instrumental modules of this phase, illustrated in Figure 3 with green boxes, are the tools employed for deterministic Flight Plan Optimization (FPO) and deterministic Trajectory Prediction (TP). The former will allow for the optimization of the trajectories to be followed starting from an initial flight plan, so that the dataset feeding the process for calculating the collocation points required to fit the aPCE polynomials is constituted of optimized trajectories. The latter allows for the calculation of the trajectories that are needed in order to fit the coefficients of the aPCE polynomials. The characteristics and details of both tools are explained in Section 3.1.2 and Section 3.1.4 respectively, with an introduction to how the trajectories will be modelled in Section 3.1.1, and the calculation process and purpose of the mentioned collocation points are commented in Section 3.1.3.

### 3.1.1 Trajectory modelling

The flight plan optimization activities to be described in Section 3.1.2, as well as the trajectory prediction tasks to be described in Section 3.1.4, will be executed using the DYNAMO software [27]. In order to understand how this software handles the trajectories to be computed, it will be important to establish the basis for understanding the processes to be followed when modelling trajectories in both the optimization and the prediction tasks.

DYNAMO software is the UPC in-house trajectory prediction and optimization software. This software has been made available to the project and it has been integrated into the developed framework to compute the trajectories required to fit the aPCE polynomials.

The trajectory computation starts at 50ft above the departure runway elevation with landing gear up and flaps/slats in take-off configuration and ends at 50ft above the destination runway elevation with landing gear down and flaps/slats in landing configuration. Considering the needs for the START project, it was proposed to model the trajectory in the vertical domain as a sequence of the following flight phases:

- Take-off and initial climb (block of several phases): A predefined sequence of aircraft intent instances and hypotheses have been implemented.
- A first block with a predefined sequence of phases with a predefined pair of aircraft intent instances per phase is implemented first. Therefore, all phases within this block are not subject to optimization since the movement of the aircraft in the vertical plane is completely constrained by the two predefined aircraft intent instances. The first phase is executed at maximum take-off thrust with flaps/slats in take-off configuration. Once the thrust reduction altitude is reached, the maximum engine rating is switched to maximum climb. Then, a sequence of phases follows to progressively accelerate the aircraft and retract flaps/slats. This block of phases ends when the aircraft is in clean configuration. It is worth noting that what is fixed in this block are the aircraft intents (i.e., initial climb speed), but not their specific values (i.e., 170 knots). Different aircraft types, different aircraft weights and different weather conditions might lead to different specific values for those intents. Similarly, the “take-off” flaps/slats configuration used here will be aircraft model dependent. Thus, although this block is not optimised, the particularities of the flight are taken into account and different initial climbs will be obtained for different aircraft/masses/weather.
- Clean climb below FL100: A small phase follows to accelerate the aircraft to 250 knots calibrated airspeed (CAS) or ECON CAS, whatever the smallest speed is. The ECON CAS is the “economic” speed, resulting from the optimization process. This speed is such that the compound optimization function is minimised which takes into account fuel consumption and flight time (see section 3.1.2). Then, a constant CAS climb at maximum climb thrust follows up to reaching FL100. In this way, the typical ATM restriction of maximum 250kt CAS below FL100 is modelled here, except for those (rather exceptional) cases where the optimal climb CAS is below 250kt where the speed constraint is not applicable.
- Climb at constant CAS: Above FL100, and assuming a given throttle setting (i.e., maximum climb thrust), the optimiser computes the optimal speed (ECON speed) and the aircraft flies at this speed until the ECON Mach is reached (optimal Mach climb also computed by the

optimiser). If needed, a small phase of acceleration from 250 knots to the ECON CAS is added before. For trajectory prediction the value of CAS value and thrust should be provided as input.

- Climb at constant Mach: Assuming a given throttle setting (i.e., maximum climb thrust), the optimiser computes the optimal Mach (ECON Mach) and the aircraft flies at this Mach until the optimal first cruise altitude is reached. Thus, the final altitude of this phase defines the Top of Climb (TOC) value. A short acceleration phase at the end of the climb could be to reach the cruise Mach. For trajectory prediction, the values of Mach and thrust setting should be provided as input.
- Cruise (block of several phases): Assuming a finite sequence of constant Altitude and Constant Mach segments. The optimiser determines the optimal Altitude-Mach values, taking into account a given maximum thrust rating (i.e., maximum cruise thrust) while in case of trajectory prediction it should be provided as input.
- The trajectory can contain several step climbs (i.e., changes in the cruise altitude), which should be provided as intents to perform the trajectory prediction. But it will be the optimiser who will determine the best number of step climbs (that could be zero) and the exact location of each step climb, while observing the following constraints (configurable):
  - A minimum cruise of 50 nm and 5 minutes is enforced before the next step climb.
  - Altitude steps of 2000 ft
  - During the whole step climb the aircraft shall maintain, at least, 500 ft/min of rate of climb (ROC). Otherwise, the step climb is disregarded.
  - A given throttle setting is assumed (i.e., maximum climb thrust)

It should be noted that the small climb segment that goes from a cruise altitude to the next one is also modelled, taking into account the dynamics of the aircraft in the same way they are considered for the rest of the trajectory. The final altitude of this block of phases defines the Top of Descent (TOD) value (i.e., the altitude of the last step climb).

An acceleration/deceleration phase could be required to move from cruise Mach to Descent Mach speeds.

- Descent at constant Mach: Assuming a given throttle setting (i.e., idle thrust), an initial descent phase is executed at constant Mach. Similar to the climb, the optimiser computes the ECON Mach for the descent. This phase ends once the descent ECON CAS is reached. For trajectory prediction the value of Mach and thrust (or idle thrust) should be provided as input.
- Descent at constant CAS: Assuming a given throttle setting (i.e., idle), the optimiser computes the ECON CAS for the descent. This phase ends when reaching FL100. Clean descent below FL100: like in the climb, the speed is limited to 250 knots CAS below FL100. Thus, if the ECON descent CAS is above 250 knots a deceleration is executed to 250 knots and the idle descent continues at this speed. For trajectory prediction, the value of ECON CAS and thrust (or idle thrust) should be provided as input.
- Approach and landing (block of phases): Like in the take-off and initial climb block, a predefined sequence of phases with a predefined pair of aircraft intent instances per phase is

implemented to model a progressive flaps/slats extension, the interception of the Instrumental Landing System (ILS) glide slope, gear down deployment and a progressive deceleration to the final approach speed. Thus, this block of phases is not subject to optimization, but the exact values for speeds and flap/slats settings will be aircraft/mass/weather dependent.

Since the starting reference point is the runway threshold of the origin airport, both the distance and time are computed as the elapsed time and flown distance from that point. Push-back and taxi out, plus taxi-in and parking are not computed.

As stated in the phase descriptions above, it is required to provide some data in order to compute the trajectory prediction.

### 3.1.1.1 Main input parameters

The main input parameters that are considered in DYNAMO to optimise or predict trajectories are:

- Mass of the aircraft (for both trajectory prediction and optimization). This value has to be defined, or a default value is taken. In START project, this value has been defined as 80% of Maximum Landing Mass of the A320-231.
- Weather: wind, pressure and temperature (for both trajectory prediction and optimization). Based on GRIB format, the weather information should be provided for the day and time of the prediction/optimization. In case the requested day and time are not available in the database, DYNAMO will take the closest weather information available. Weather input must be provided following GRIB/GRIB2 format. If the weather information is coming from a forecast or a nowcast is not a relevant issue for DYNAMO.
- Cost Index (only in optimization). Cost Index (CI) value must be defined, or a default value is taken. In START project CI equal to zero has been selected so far, although it is planned to use real CI values in a later stage.

### 3.1.1.2 DYNAMO output

Both the flight plan optimizer and trajectory prediction tools will provide a trajectory as a result based on the DYNAMO software that has been particularised and further developed for the needs of the START project. Once this trajectory is available, any related parameter can be calculated:

- TOC: it is considered that the Top of Climb is that altitude that the aircraft reaches after the climb phase. It is the value obtained from the optimizer when applying the “constant altitude” and “constant Mach” constraints (basic definition of the cruise phase).
- TOD: it is considered that the Top of Descent is that altitude just before the descent phase, and just finishing the cruise phase (Constant Altitude and Constant Mach).
- TOC Distance: flown distance from the threshold of the origin runway to reach the TOC.
- TOD Distance: flown distance from the threshold of the origin runway to reach the TOD.
- TOC Time: elapsed time from the threshold of the origin runway to reach the TOC.
- TOD Time: elapsed time from the threshold of the origin runway to reach the TOD.

- Number of step climbs in cruise
- For each step climb:
  - Step climb trip distance (bottom of climb and/or top of climb)
  - Step climb elapsed time (bottom of climb and/or top of climb)

These values can be post-processed from a given trajectory (with the format of the DYNAMO output). The START project required several modifications and implementations to enable some of these parameters to be used as inputs of the Trajectory Predictor.

### 3.1.1.3 DYNAMO execution strategy

DYNAMO can be used following any of the three following options:

- Aircraft intents for all the phases are provided; DYNAMO is able to predict the trajectory.
- Aircraft intents for some of the phases are provided. Those phases not defined are taking pre-defined values, which could come from a previous optimization run or could be defined by the user; DYNAMO is able to predict the trajectory.
- Aircraft intents for a few phases are provided; DYNAMO optimizes those phases not defined by the initial intents. Compared to a previous optimization, leaving some intents free will lead to a new optimization with additional constraints (the defined intents), so the final outcome of this constrained optimization can differ from the original optimization results. Then, a few phases are fixed by the intents, the remaining are going through the optimizer, so we obtain a hybrid optimization and prediction of the trajectory.

### 3.1.2 Flight plan optimization

As it was commented above, the first phase of the proposed methodology requires the employment of a tool capable of computing the optimal trajectories for a given flight plan, declaring the intended flight to be executed for any given city pair. The proposed tool for undertaking this task is the DYNAMO trajectory optimizer.

The trajectory optimization in the vertical domain is dealing with the following phases:

- Climb at constant CAS: The aim of the optimizer is to compute the optimal CAS, with a given throttle setting (i.e., maximum climb).
- Climb at constant Mach: The aim of the optimizer is to compute the optimal Mach number, with a given throttle setting (i.e., maximum climb).
- Cruise: The optimiser will determine the optimal values for altitude and Mach number. The trajectory can contain step climbs (i.e., changing the cruise altitude). Thus, the optimiser will determine the best number of step climbs (that could be zero) and the exact location of each step climb, while observing the already mentioned constraints.
- Descent at constant Mach: The aim of the optimizer is to compute the optimal Mach number, with a given throttle setting (i.e., idle).



- Descent at constant CAS: The aim of the optimizer is to compute the optimal CAS, with a given throttle setting (i.e., idle).
- Take-off and initial climb: block of phases not subject to optimisation.
- Approach and landing: block of phases not subject to optimisation.

Excluding the take-off, initial climb, approach and landing phases, which are not subjected to optimization, DYNAMO can optimise the whole trajectory or could optimise some phases (for example, fixing the intents for the two climbs and then optimising cruise and descent, or fixing the intents for the descent and only optimising cruise, etc.). If all intents are fixed for all phases, then there is no optimisation, producing then a pure trajectory prediction.

### 3.1.2.1 Objective function

The optimizer is using a single function to minimize, named  $J$ , defined as:

$$J = Fuel + CI \cdot Time$$

With  $Fuel$  being the total fuel burnt,  $CI$  being the selected cost index and  $Time$  being the total flight time.

The  $CI$  is an input parameter for the trajectory optimization algorithm and specifies the relative importance of time associated costs with respect to the fuel cost. Thus, this is a parameter chosen by the airline taking into consideration its internal policies and cost structures. The cost index value can be a provided input, or a default value will be chosen.

### 3.1.2.2 Horizontal optimizer

Although the main application of DYNAMO on the START project is based on the vertical optimization and prediction, this section is aimed to complement what has been described so far with the settings established for the horizontal profile.

The horizontal optimizer has different modes of use:

- Set a fixed route and not optimize. Mainly defining the waypoints beforehand as in the FPL.
- Optimize based on the routes available in a graph (structured network of Air Traffic Service (ATS) routes). This graph can include Free Route Areas (FRA). The graph could represent the actual airspace, or it could be a partial modification, or it could be completely invented. The key point here is to manage to get the graph.
- Set only origin and destination and fly following the great circle distance between these two points.
- Full Free Route (no ATS routes). We call that “Full” Free Route, since current “Free Route” implementations have entry, intermediate, and exit points and we are assuming that the free route is executed directly from origin/destination airports, without considering the particularities of the terminal airspace.

### 3.1.3 Calculation of aPCE polynomial and collocation points

From the optimized flight plan dataset, the following 8 variables have been considered as input parameters for the aPCE:

- Mach number at climb phase
- CAS at climb phase
- Pressure altitude at cruise phase
- Mach number at cruise phase
- Mach number at descent phase
- CAS at descent phase
- TOC pressure altitude
- TOD pressure altitude

Note that is not necessary to use all the variables as input for the aPCE. Each of these variables has an arbitrary distribution, thus aPCE becoming indispensable to generate the appropriate polynomial basis functions describing the response of the model i.e., the trajectory prediction.

The statistical moments for each variable are computed following Equation (6), which can be used together with the orthogonal condition for polynomials posed in Equations (10)-(13) to obtain the polynomial coefficients from the linear system of Equation (14).

As shown in Section 2.2.3, the collocations points are obtained from the roots of the next higher-order polynomial for each stochastic parameter. Since the number of available collocation points is larger than the number of unknowns, the system is overdetermined. This issue is solved by selecting the optimal  $M$  combination of collocation points in terms of the probability of each combination of collocation points. This approach allows to obtain  $M$  combinations of collocation points that are transformed back into optimized flight plans.

### 3.1.4 Trajectory prediction

Trajectory prediction is based on the definition of the flight intents. A summary of intents per phase is the following:

- Climb at constant CAS: Throttle setting and CAS.
- Climb at constant Mach: Throttle setting and Mach.
- Cruise: (sequences of) Altitude and Mach
- Descent at constant Mach: Throttle setting and Mach.
- Descent at constant CAS: Throttle setting and CAS.

Other combinations of intents are also possible in DYNAMO, such as for instance “CAS and Vertical Speed” or “CAS and flight path angle”. Yet, these are typically used at tactical level and/or at low altitudes (approach etc). So, it has been considered as being out of the scope of the START project.

The specific application to START project is devoted to providing a fast response to the calculation of the trajectories defined by the collocation points extracted from the aPCE method. The specific input aircraft intent variables for the calculation of those trajectories are listed in Section 3.1.3. TOC and TOD altitude are not normally defined in the input aircraft intents but are calculated as a result of the optimization or prediction process. A special implementation for START project is enabling the definition of these two altitudes as input parameters to adjust the vertical profile.

Two different tests have been performed using all the listed intents or just using a restricted set. This restricted set includes the climb CAS and Mach number, the TOC altitude and the cruise altitude.

Other data included as parameters from each collocation point include the airport of departure and of arrival, so that the trajectories can be computed for a specific city pair.

The definition of the collocation points could lead to unfeasible flight intents, which is unacceptable from a mathematical point of view. Since the aPCE method requires the evaluation of all the points in order to estimate the statistical parameters, not getting all the collocation points evaluated would lead to a complete failure of the method.

The trajectory prediction software checks for these infeasibilities, as well as other vertical profiles issues; namely the ordering of the step climb/descent during the cruise phase. It has led to the definition of several cruise types:

- Cruise block of type 1: 3 different altitudes. Two consecutive step climbs. The collocation points are defining 3 different altitudes, which defines a consecutive climb. Due to the requirements imposed on the cruise phase, a minimum separation (distance and time) between each step climb is considered. The ROC should be also checked to ensure that the plane is capable of performing the required operation. In case the aircraft performance is not enabling a minimum ROC, DYNAMO will enlarge the previous phase until the characteristics and performances of the airplane enable a ROC value which fulfils the requirement. If this situation is not reached before arriving at the point of the TOD altitude, the corresponding step climb will not be executed.
- Cruise block of type 2: 3 different altitudes. Step descent followed by a step climb. Although it can hardly represent real cruise operations, inputs from the collocation points can lead to the definition of a cruise altitude below the TOC altitude, with a second step climb before the descent phase. As described on the previous cruise type, separation between steps and ROC requirements will be checked. If some of them are not fulfilled, then, the step is not executed.
- Cruise block of type 3: 3 different altitudes. Step climb followed by a step descent. A standard definition of the cruise altitude from a theoretical point of view, with an initial step climb, followed by a step descent. Separation between steps and ROC values will be assessed before forcing the execution of the operation.
- Cruise block of type 4: 3 different altitudes. Two consecutive step descents. For such a case, where two step descents are defined, the only requirement to be fulfilled is to ensure a minimum separation between the two steps.

- Cruise block of type 5: TOC altitude equal to cruise altitude and one step climb. This scenario represents a simplification compared to cruise block type 1, since it still defines a step climb along the cruise phase, but the initial cruise altitude and the first step climb altitude are the same. Again, separation between steps and ROC are checked for requirements fulfilment.
- Cruise block of type 6: One step climb and cruise altitude equal to TOD altitude. It is similar to the cruise block of type 5 but inverting the equalities. The final result is a similar profile, although it is the cruise and the TOD altitudes that are equal.
- Cruise block of type 7: One step descent and cruise altitude equal to TOD Altitude. Another situation that provides a similar profile that type 5 and 6 but considering a descent step instead of a climb step.
- Cruise block of type 8: TOC altitude equal to cruise altitude and one step descent. Similar to type 8, so similar to 5, 6 and 7, but starting with the same altitude as the TOC altitude and applying a descent step. Since it is a descent, ROC requirement is not applicable.
- Cruise block of type 9: One single cruise altitude. The simplest case, which equals the three altitudes, so the cruise phase starts at TOC and ends at TOD altitudes, being both the same.

All these types of cruise block have to fulfil the requirements of the cruise phase, as defined in the trajectory modelling basis described in Section 3.1.1.

These cruise types have been defined considering the specification in the collocation points of three altitudes, namely the TOC, cruise and TOD ones. If the collocation points are modified only defining the TOC and cruise altitudes, the number of cruise types will be reduced, but the concepts described above will remain the same.

In order to ensure the feasibility of the flight, additional checks are done while defining the vertical profile:

- If the TOC altitude is lower than the altitude of the climb Mach phase, so the TOC altitude is below the cross-over altitude of the given climb Mach number and CAS, this climb Mach phase is not considered.
- Same situation is considered during descent and with regards the TOD altitude.
- If ROC available at TOC altitude is not larger than 500 ft/min this altitude is disregarded and the TOC altitude is the first available FL where a minimum ROC available of 500 ft/min can be attained.
- Flight envelope protection: Maximum operating Mach number (MMO), maximum operating speed (VMO) for maximum speeds, *Greendot* (CAS) for minimum speed. If a higher/lower speed is given as intent, then it is disregarded, and the max/min limit is imposed.

### 3.1.5 Retrieving the aPCE coefficients

Once the trajectories corresponding to the previously defined collocation points are obtained from the trajectory-prediction module, aPCE coefficients for Equation (1) may be obtained. For that purpose,

the least-square-approximation method will be used. Equation (16) can be expressed in matrix form as follows:

$$\mathbf{B} = (\mathbf{\Gamma}^T \mathbf{\Gamma})^{-1} \mathbf{\Gamma}^T \mathbf{Y} \quad (23)$$

where  $\mathbf{B}$ ,  $\mathbf{\Gamma}$ , and  $\mathbf{Y}$  are the matrices of coefficients, polynomials and outputs respectively. Note that bold uppercase letters refer to matrices. The aPCE polynomials previously obtained are evaluated at each collocation points, thus leading to the composition of matrix  $\mathbf{\Gamma}$ . Matrix  $\mathbf{Y}$  is generated from trajectory information. Since the present aPCE implementation intends to provide an uncertainty evolution with respect to the time, for each sample i.e., for each row of  $\mathbf{Y}$ , there is more than one column. Each column contains the flight time up to a single predefined point in the horizontal path of the route, for example at the 25%, 50%, 75% and 100% covered distance with respect to the entire one. Note that Equation (14) posed a system linear of equations that requires a matrix inverse to be solved. Depending on the polynomial degree this matrix could be ill-conditioned, which would lead to completely wrong results. Whereas in the cases of study that condition does not happen, Moore-Penrose algorithm is used to compute the inverse. This algorithm allows to reduce significantly the numerical error associated to ill-conditioned matrices.

### 3.1.6 Integration of weather information

Similar to Section 3.1.3, POD coefficients or CNN-AE latent variables are added to the list of input parameters in the aPCE. In the present study, 3 coefficients are considered. For the aPCE fitting purpose, weather data for years 2016 and 2017 are considered. The weather is downloaded from European Center for Medium-Range Weather Forecasts (ECMWF) in a rectangular grid that covers the area between the origin and destination airports. The sides of this grid are aligned with the meridians and parallels.

Once the set of collocation points are obtained, the weather coefficients are transformed back into weather information with physical dimensions. Note that each combination of collocation points is combined with their corresponding weather. It is worth mentioning the standard format to operate with weather information is known as GRIB. While there is full support to read this format from the ECMWF, the writing support is quite limited.

The generated flight plan and weather information for each combination of collocation point is fed into the trajectory predictor. With the generated output, and the aPCE polynomials evaluated at each combination of collocation points, it is possible to obtain the aPCE coefficients.

### 3.1.7 Uncertainty quantification of input variables

Parallel to the process previously described of obtaining the definition of the aPCE polynomials, the quantification of the uncertainty for the aircraft intent variables is executed in this first phase of the framework. This specific module is implemented in this phase because it uses the same data inputs than the ones used for the determination of the aPCE polynomials, namely, the historical instances of network demand data, consisting of flight plans and surveillance information.

As it was widely described in [2], the process for quantification of the uncertainty present in the aircraft intent variables will be executed by evaluating the differences between the planned and the actual values for these variables in past aircraft trajectories relevant for the proposed scenario (i.e., for any given city pair, aircraft type, etc.). Hence, this process is fed by the datasets available in this phase of

the process, which will therefore be evaluated in order to obtain the probability distributions for the observed differences in the values of the identified uncertain aircraft intent variables. These probability distributions will later be employed in order to define the possible perturbations in the defined uncertain variables within the second phase, and therefore will be paramount in order to define the spectrum of values of the output probabilistic trajectory variables.

### 3.2 Probabilistic trajectory generation

The second phase of the framework can be implemented at any point in time once the first phase has been completed and the definition of the relevant aPCE polynomials has been established. The expected framework for this second phase is to be used in the tactical phase, in conjunction with all the other activities to be executed within the START project. This is because the modules deployed within this second phase of the methodology are prepared to consume network demand information as it is issued and calculate the set of probabilistic trajectories that can be incurred when following it, taking into consideration the potential perturbations that it may suffer along its execution.

The schema for the proposed methodology to be followed is represented in Figure 4. As it can be observed, both the weather processing module and the aPCE polynomials, computed within the first phase of the framework, constitute an integral part of the process for obtaining the desired probabilistic trajectories. Regarding the input, the same kind of information as the one commented for the first phase will be employed, although in this second phase, the information is to be consumed through a live feed, so that current data relevant for the short-term future (following the framework proposed by the START project) is expected regarding the scenario of interest.

Additionally, three further modules, represented in green colour in Figure 4, are required in order to perform all the necessary calculations. The first one is the module for executing the deterministic optimization of the flight plans that are gathered in the tactical phase. This optimization is executed following the same procedure as the one described in Section 3.1.2, just in order to have the same kind of input than the one employed for the calculation of the aPCE polynomials. Also, the uncertainty distributions computed for the aircraft intent variables as explained in Section 3.1.7 will be integrated in order to retrieve the necessary perturbation values for the uncertain input variables on which the aPCE polynomials depend. This is the key step that allows the deployed methodology to account for the potential deviations that the flight may suffer with respect to the declared plan, as observed in similar flights in the past. Finally, the data assimilation models, presented in [2], are integrated in this phase in order to receive updated information about the current air traffic status that may affect the flight in its execution. Therefore, these updates will be taken into account in order to reduce the uncertainty in some of other input values that influence the probabilistic trajectories to be obtained.

In order to describe the processes executed within the modules presented in Figure 4, the optimized flight plan will be taken as initial point, consumed in its declared version from a live feed (as established in [28]) and optimized following the process described in Section 3.1.2. Then, Section 3.2.1 will explain how, using the weather processing module and the uncertainty distributions coming from the first phase, the initial values for the input variables as calculated from the optimized flight plan will be perturbed to account for their actual uncertainty, and thus will constitute different input cases to be fitted into the aPCE polynomials. Once fitted, Equation (7) can be solved for each of the input cases to retrieve the corresponding values for the variables defining the aircraft trajectory. Therefore, each of the input cases will provide a different description of the final trajectory that could be described by an aircraft executing the declared flight plan. When considering all these cases together, a probability

distribution of the possible values to be adopted by the different aircraft trajectory variables will be obtained, and thus the required probabilistic trajectory set will be defined for the considered declared flight plan. Finally, Section 3.2.2 will comment on the possibility of integrating the values obtained from the data assimilation models in order to reduce the uncertainty of certain factors that affect the aircraft trajectory.

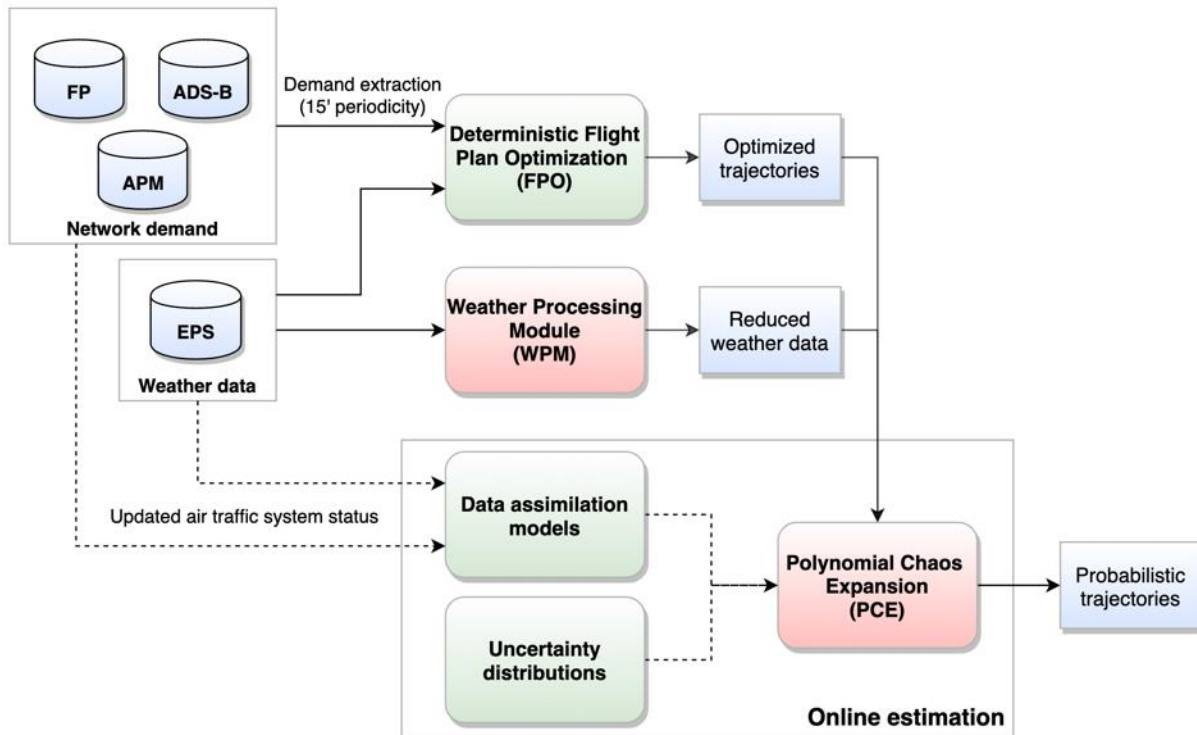


Figure 4 Structure for the generation of probabilistic trajectories from demand data

### 3.2.1 Perturbations for aPCE polynomials input

Once the optimized flight plan is retrieved, a definition of the declared values for the aircraft intent variables is obtained for the nominal trajectory that the aircraft will have to describe. However, as it was made evident throughout this document, deviations from the plan normally occur on all aircraft trajectories when the flight is executed. As such, the objective of this framework is to account for the possible spectrum of deviations and project the probabilistic trajectories that may be incurred from the nominal one established by the declared flight plan.

The proposed methodology will be then to perturb the nominal values for the aircraft intent variables considering the potential deviations that can be expected on them. These perturbations will be obtained by following a data-driven approach by which comparable past trajectories are observed in order to derive the probability distributions of the deviations incurred in these variables in historical instances. The process to obtain these probability distributions was described in Section 3.1.7, and now they will be used to define the spectrum of perturbations to be considered.

Consequently, the procedure for perturbing the nominal values for the aircraft intent variables is adding and/or subtracting the typical deviations observed in past similar trajectories. The criteria for defining the range of values for these deviations is arbitrary but should cover the wide majority of

possibilities. Extreme cases in which the deviations are very large may be avoided, as depending on the magnitude of cases considered, they may be statistically irrelevant.

With this procedure, the uncertainty in the values for the aircraft intent variables is considered in the calculation of potential trajectories to be incurred. Each combination of perturbed values for each of the aircraft intent variables will lead to a unique trajectory. Thus, all the calculated trajectories will conform a set of probabilistic trajectories emanating from a single flight plan.

### 3.2.1.1 Weather

Weather perturbations are included in the model by means of ensemble weather forecast datasets retrieved from the ECMWF's Ensemble Prediction System (EPS). These forecasts are composed of a reference forecast, known as control forecast, as well as up to 50 perturbed cases to this nominal forecast, following the perturbation methodology introduced in [2].

Therefore, the procedure for integrating these perturbations to the weather conditions consists of calculating the predictions for the entire set of aircraft intent variables' perturbations with each of the perturbed weather forecast. Consequently, all these combinations of perturbed cases provide a set of individual trajectory estimations that conform a probability value distribution for the trajectory variables of interest.

### 3.2.2 Data assimilation models

Further input information can be considered within the proposed framework in order to enhance the consideration of micro-level uncertainties in the proposed methodology. In particular, the data assimilation models presented in [2] can be integrated within the second phase of the framework. These models provided different information:

- A runway configuration model was introduced capable of estimating the runway from which any flight would depart from a given airport based on the wind information available in the airport weather forecasts (Meteorological Aerodrome Reports (METAR) from National Oceanic and Atmospheric Administration (NOAA)).
- A taxi time model was introduced capable of estimating the time it would take any given aircraft departing from any given airport to complete the taxiing phase from the parking to the runway based on the surveillance reports being received from a live feed.
- A turnaround time model was introduced capable of estimating the time it would take any given aircraft to complete the turnaround phase (from the aircraft entering a parking spot in the arrival phase of a previous flight to exiting the same parking spot in the departure phase of the immediate next flight to be served by the same aircraft) based on the information contained within EUROCONTROL's DDR2 dataset. With the turnaround time estimation and the actual arrival time for the previous flight, an estimation can be done on the off-block time for the departure operation.

All these models can provide estimations on relevant factors that could affect any given flight planned to depart in the short-term future. Following the pre-tactical temporal framework proposed within the START project, this would mean that the estimations provided by these models could be used for all those operations planned to depart in the immediate hours after the execution of the second phase of the framework.



Including the estimates provided by the proposed data assimilation models can help in reducing the uncertainty associated to certain factors or parameters affecting the trajectory. These factors would be in this case the initial conditions of the flight, as using the estimates for the runway to be used and for the off-block and taxi time for the flight could eliminate the uncertainty on the initial time and location of the flight. This would consequently introduce some prediction errors in the calculation, as the issued estimates will not be accurate each and every time.

An important factor to take into account is the fact that assuming an initial location and time for the flight would theoretically require the declared flight plan to be optimized taking into account this new information. This is because the optimal calculation of the nominal trajectory to be followed based on the declared flight plan would change based on both a different initial location (starting the flight from a different runway than the one declared in the flight plan would probably lead to a different lateral and horizontal profile to be followed by the aircraft) and a different initial time (starting the flight at a different time than the one declared in the flight plan, with a different taxi time, would maybe cause the aircraft to be affected by different weather conditions, and therefore would maybe make it follow a different lateral or horizontal profile). Although this consideration will not be explored in the study case shown in Section 4, it would be interesting to observe the trade-off caused in the accuracy of the probabilistic trajectory determination when accounting for the estimates issued by the data assimilation models.

## 4 Use case

---

The objective of this section is to exemplify the framework proposed in Section 3 in order to obtain a probability distribution of values for any given aircraft trajectory variable as a result of the consideration of potential uncertainty in the identified set of input variables affecting the trajectory prediction process. The use case developed during this section will therefore comment on all the steps to be followed for both phases of the framework, first in order to obtain the definition of the aPCE polynomials that allow for the description of the aircraft trajectory variables of interest as a function of the considered uncertain input variables, and then to retrieve the probability distributions for those trajectory variables attending to the potential perturbations to be taken into account.

It is established that for this use case, the flight time will be the trajectory variable to be evaluated, specifically at the end point of the trajectory. The flight time is selected because it is the trajectory variable that allows for a straightforward comparison to similar values obtained by using the trajectory prediction tool or by observing the flown trajectories, and also because it will be the variable of interest for later stages of the START project. The temporal and spatial framework for said evaluation will be established on all flights covering the route between Adolfo-Suárez Madrid Barajas airport (LEMD) and Franz Josef Strauss Munich International Airport (EDDM) during June 2018, for all present airlines and aircraft types.

As it was represented in Figure 3, the main input datasets to be considered are conformed by network demand and weather data. The sources from where this information will be consumed were already identified on the Data Management Plan [28], and are specific to each data piece. Flight plans will be gathered to be consumed by the flight plan optimization module from EUROCONTROL's Demand Data Repository (DDR2) in the ALLFT+ format, in their filed version. Surveillance data are compiled in order to perform the uncertainty quantification for aircraft intent variables from BDG's data pool, which consumes surveillance messages from Flightradar24. Aircraft performance models to be used throughout the different tools deployed in the proposed framework come from EUROCONTROL's BADA4 [29]. Regarding weather information, the ERA5 reanalysis datasets from ECMWF will be employed in the first phase to have a better weather conditions definition. Although the ECMWF's EPS are proposed in Section 3.2.1.1 as a mean to consider weather perturbations in the second phase of the methodology, they are not employed in this study case. As an alternative for the sake of simplicity, ERA5 reanalysis datasets are employed as well. A more detail explanation about this will be provided in Section 4.2

The proposed use case was scaled progressively in terms of complexity, and as such will be documented throughout this section. First, a complete study of the process followed will be done in Section 4.1 considering only aircraft intent uncertainties, disregarding uncertainty in the micro-level coming from other sources. Then, in Section 4.2, it will be described how the uncertainty in the weather conditions could be included in the process, and Section 4.3 will comment on how uncertainty on the initial flight time could be added by employing the outputs provided by the proposed data assimilation models.

### 4.1 Considering aircraft intent uncertainties

The process to be executed in order to obtain the probability distribution of possible flight times for the trajectories to be incurred by following any given declared flight plan will follow exactly the

schemas shown in Figure 3 and Figure 4. In this first iteration, only the potential uncertainties coming from the aircraft intent definition will be considered, so weather and initial conditions are momentarily disregarded.

As it was documented in Section 3, the process starts by optimizing the trajectories corresponding to the declared flight plans following the process described in Section 3.1.2 for a relevant timeframe regarding the scenario of interest. For this purpose, 2731 flight plans declared for the flights between LEMD and EDDM were collected and optimized for the period between June 2017 and May 2018. These optimized trajectories constitute the baseline for the calculation of the collocation points for all the uncertain aircraft intent variables to be considered, and thus for the first step of the definition of the aPCE polynomials, as explained in Section 3.1.3. In this first iteration, there will be 8 different aircraft intent variables for which their potential uncertainty will be considered: two for the climb and descent phases (calibrated airspeed and Mach number), another two for the cruise phase (pressure altitude and Mach number), as well as the altitudes achieved at the TOC and TOD. The value distributions over all the considered optimized trajectories for these 8 aircraft intent variables are shown in Figure 5. These histograms illustrate the possible range of values to be adopted for these variables over similar trajectories, and from them, the value spectrum for the calculation of the collocation points is established. In general, this spectrum will cover a range smaller than the one covered by considering the standard deviation and is tailored to keep reasonable values for all variables. This considered range of values is marked in Figure 5 as the one between the dashed yellow lines.

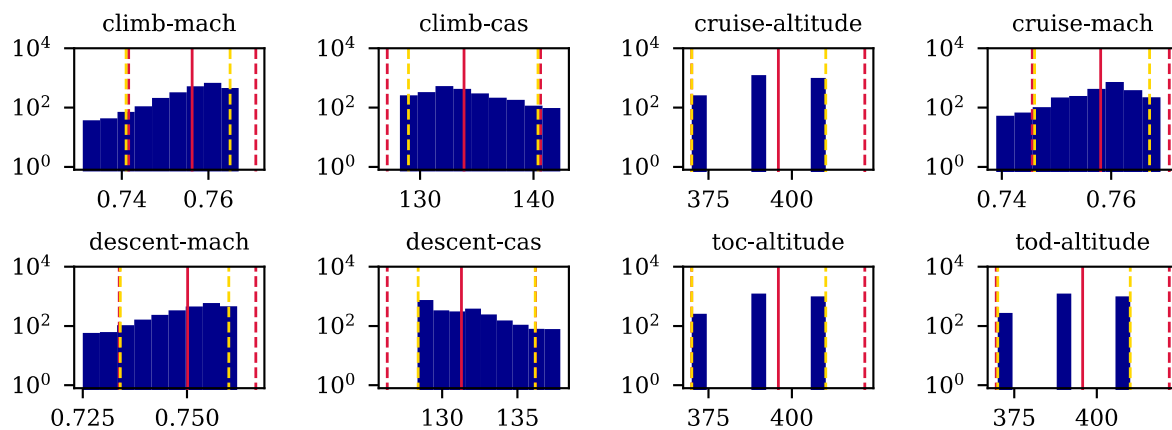


**Figure 5** Histograms of values of the considered aircraft intent variables for all optimized LEMD-EDDM trajectories between June 2017 and May 2018. Calibrated airspeeds are provided in knots, pressure altitudes in FL. Solid red lines indicate mean values, dashed red lines indicate the values for the standard deviation. Dashed yellow lines indicate the range of values considered for the calculation of the collocation points.

The calculated collocation points for an aPCE polynomial of order 3 are shown in Table 3. Following the formula established in Equation (5), in which the number of variables  $N$  considered is 8 and where the degree of the polynomial  $d$  is 3, a total of 165 combinations of values are obtained. Therefore, the TP tool will have to calculate the trajectories that comply with each of the variables' combinations in order to have the required elements to perform the polynomial fitting. The process for calculating these trajectories was described in Section 3.1.4. Once the trajectory prediction tool calculated the trajectories corresponding to the aircraft intent variables indicated, the coefficients of the aPCE polynomials can be calculated following Equation (16). This calculation completes the definition of the aPCE polynomials for the selected use case.

**Table 3: Values for the calculated collocation points for all LEMD-EDDM trajectories between June 2017 and May 2018**

$CAS_{climb}$ [kts]	$M_{climb}$	$H_{TOC}$ [ft]	$M_{cruise}$	$H_{cruise}$ [ft]	$H_{TOD}$ [ft]	$M_{desc}$	$CAS_{desc}$ [kts]
141.15	0.764	41006	0.769	41521	41005	0.759	137.03
137.01	0.756	40765	0.762	41006	39801	0.751	133.93
132.59	0.745	38990	0.753	38990	38991	0.739	131.04
129.21	0.733	37001	0.742	37001	37001	0.728	128.63

Regarding the uncertainty quantification for the considered aircraft intent variables, the process is executed following the methodology described in [2]. Therefore, the planned values for these variables are retrieved from the filed flight plan information, while the actual values are retrieved from the analysis of the trajectories present in the surveillance data for all flights between LEMD and EDDM during the considered period (June 2017 to May 2018). These differences in the selected aircraft intent variables build to distributions of the deviations between planned and flown trajectories, and therefore provides a certain insight on the dimension of the uncertainty to be expected on the selected variables.

The obtained probability density functions for all the aircraft intent variables in consideration are presented in Figure 6 and Figure 7. In general, the differences observed respond to expected behaviour. The climb and descent phases seem to be usually executed slower than what was planned, which could be argued as a will to reduce the fuel burnt. Also, differences for the TOC and cruise altitude are in intervals of 2000 feet, which was expected since rules for Air Traffic Flow Control indicate that flights going in a similar orientation (from west to east or vice versa) should be separated in altitude intervals of that magnitude. For the TOD altitude, these differences are not that well grouped in said intervals, although this could be explained by the difficulties in determining the exact point for the TOD, as its identification is complex. Finally, the velocity acquired during the cruise phase, as it can be seen in the top left plot of Figure 7, tends to be higher during the cruise phases of the actual flights.

Once the probability distributions for the deviations in the established aircraft intent variables are retrieved, as well as the definition of the aPCE polynomials is completed, the second phase of the developed methodology can be implemented. This second phase, as described previously, is the one in charge of issuing the probability distributions for the expected flight time of any given flight plan as a function of the uncertainty to be observed in the defined variables. The selected dataset for the evaluation of the results provided by the developed methodology will be all flights between LEMD and EDDM during June 2018, which amounts to a total of 202 trajectories. In order to assess the validity of the developed method, the perturbations to be introduced to the eight aircraft intent variables on which the aPCE polynomials depend have to be selected. The deviations to be expected between their values as provided in the flight plan and as flown in actual trajectories were illustrated in Figure 6 and Figure 7 for a relevant period of time, so these probability density functions will serve as the baseline from which the perturbations will be calculated.

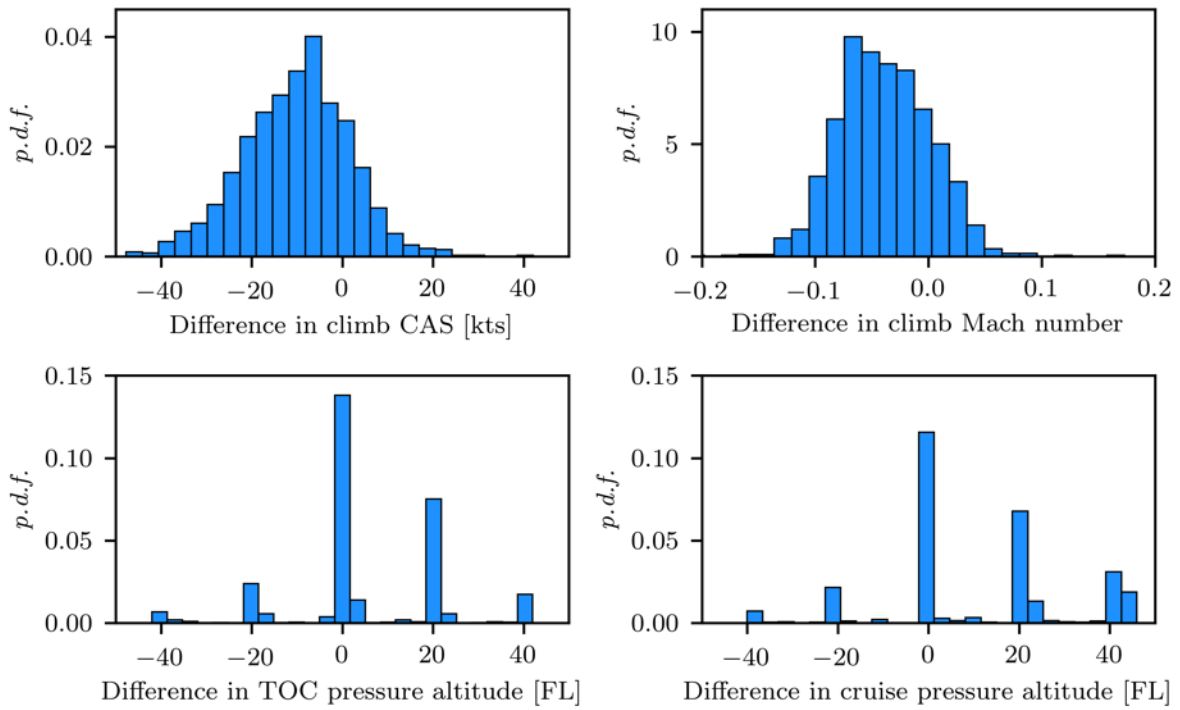


Figure 6 Probability density function of the difference between planned and observed values for the first block of aircraft intent variables

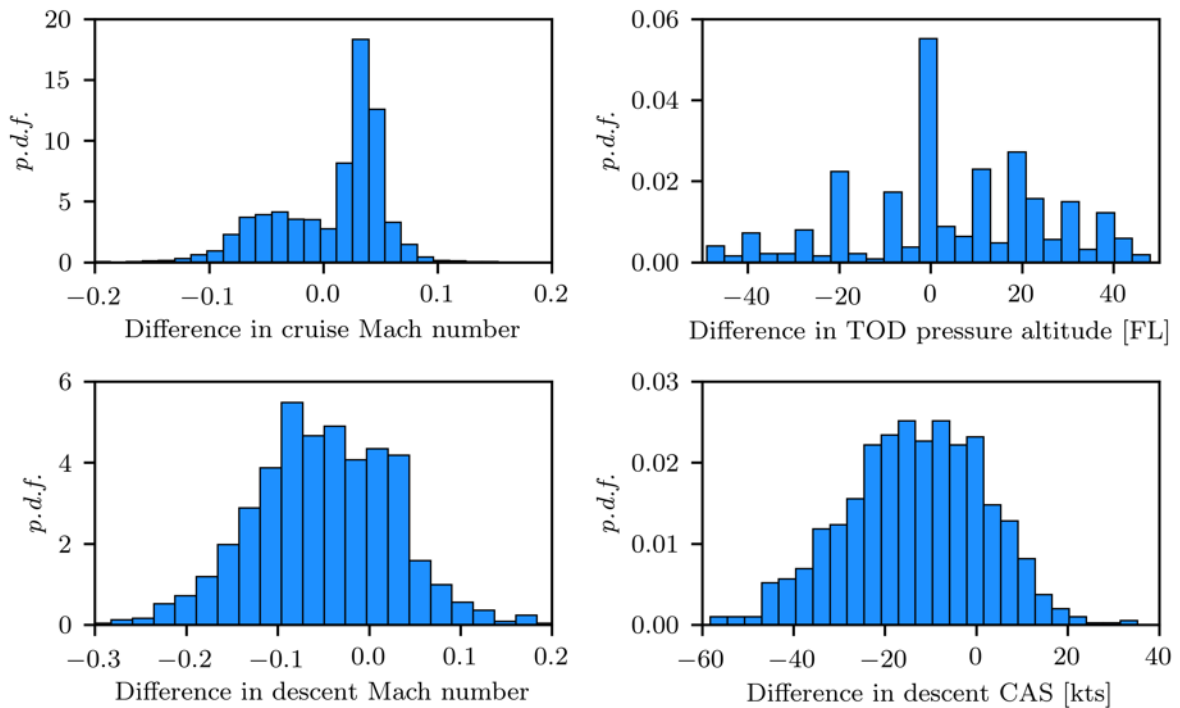


Figure 7 Probability density functions of the difference between planned and observed values for the second block of aircraft intent variables

**Table 4: Values for the perturbations introduced to the aircraft intent variables for all flights between LEMD and EDDM during June 2018**

$CAS_{climb}$ [kts]	$M_{climb}$	$H_{TOC}$ [ft]	$M_{cruise}$	$H_{cruise}$ [ft]	$H_{TOD}$ [ft]	$M_{desc}$	$CAS_{desc}$ [kts]
±19.22	±0.051	±2000	±0.056	±2000	±2000	±0.307	±62.13

In a first approach, most of these distributions can be approximated to a normal one, so we can consider their standard deviation as a good indication of how far the perturbations in the input value can be taken. However, for the TOC and cruise pressure altitude, it was already mentioned how the deviations were clearly grouped in intervals of 2000 feet, so this value will be taken instead of the standard deviation.

With the perturbations defined and the input flight plan information ready, the aPCE polynomials can provide the desired values that will build the probability distribution for the flight time. It has to be understood that, for each flight to be computed, 3 different values (nominal one and the two perturbation values as per Table 4) will be considered for each of the 8 aircraft intent variables.

For the 202 trajectories included in the present case of study, aPCE returns only a successful evaluation for 153 of them. The non-evaluated predictions suffer from numerical instabilities, which lead to unrealistic predictions. This is one of the major drawbacks of aPCE implementation, which is intimately related to its main advantage. Since aPCE allows a much lower computational cost compared to a Monte Carlo approach, the proposed optimal collocation points do not cover all the possible parametric space that can be found in the set of testing flights. Subsequently, the aircraft intent variables found in the non-evaluated cases are in regions of the parametric space very far from those evaluated with the optimal collocation points.

In order to assess the suitability of the issued flight time estimations, the actual flight times for the 202 flights considered during June 2018 are introduced in Figure 8. These are the baseline values that the issued estimations should approximate to. Therefore, a comparison of the flight times issued by the input of the flight plan data and the correspondent perturbations with these real flight times is necessary to understand how well the developed methodology replicates the real conditions. Consequently, Figure 9 is introduced illustrating this comparison for all the estimations executed with the built aPCE polynomials, showing the error incurred for each estimated flight time of each flight.

As it can be observed in Figure 9, the results are quite satisfactory, showing a normal distribution of the error centred around zero, so a large proportion of the estimations issued are accurate with respect to reality. The dispersion of the results acquires a maximum value of around 20 minutes of deviation, a magnitude not very disproportionate for a flight that normally takes around 125 minutes as shown in Figure 9, so in the worst cases the estimation is off by a 20% percent. These inaccurate estimations correspond to cases in which the perturbations included for some of the uncertain aircraft intent variables deviate too much the trajectory from the normal course, and therefore lead to a final estimation of the flight time that is off with respect to the incurred one.

It is also interesting to observe how the issued estimations with the aPCE polynomials compare to the ones that a normal trajectory prediction tool would issue for the same scenario. This comparison is introduced with Figure 10, where the probability density functions of the issued flight times for the

proposed scenario by both the trajectory prediction tool (described in Section 3.1.4) and the built aPCE polynomials are shown. It is seen that the trajectory prediction tool also does a good job of estimating the flight times, and even the dispersion obtained is closer to the one observed in reality. These more extreme cases are not properly calculated with the aPCE polynomial cause they probably are related to more extreme flight conditions in which the computation of the polynomials fail, as previously mentioned.

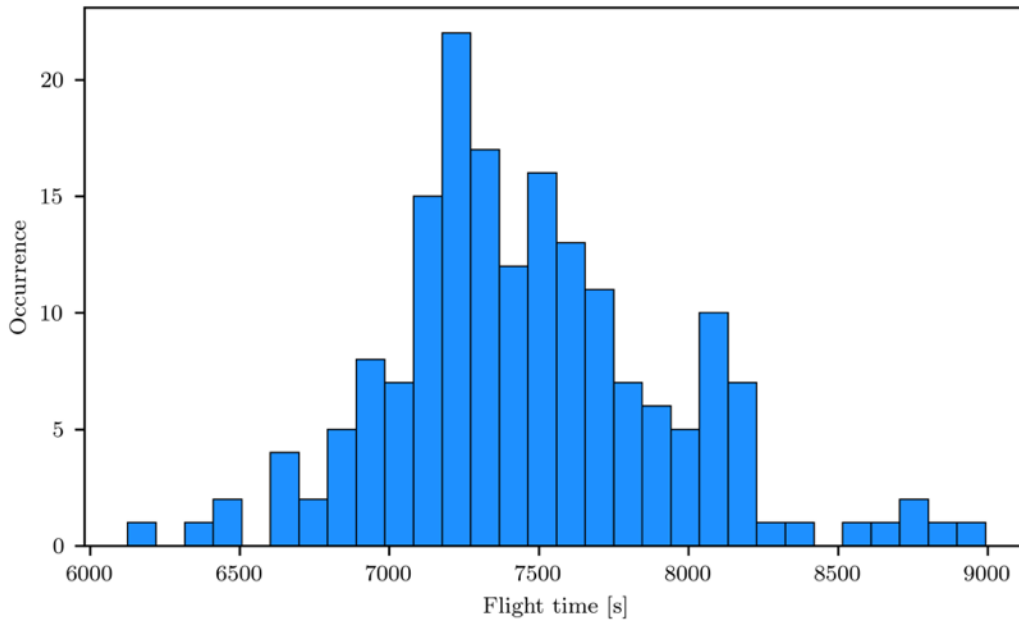


Figure 8 Histogram for the real flight times for all flights between LEMD and EDDM during June 2018

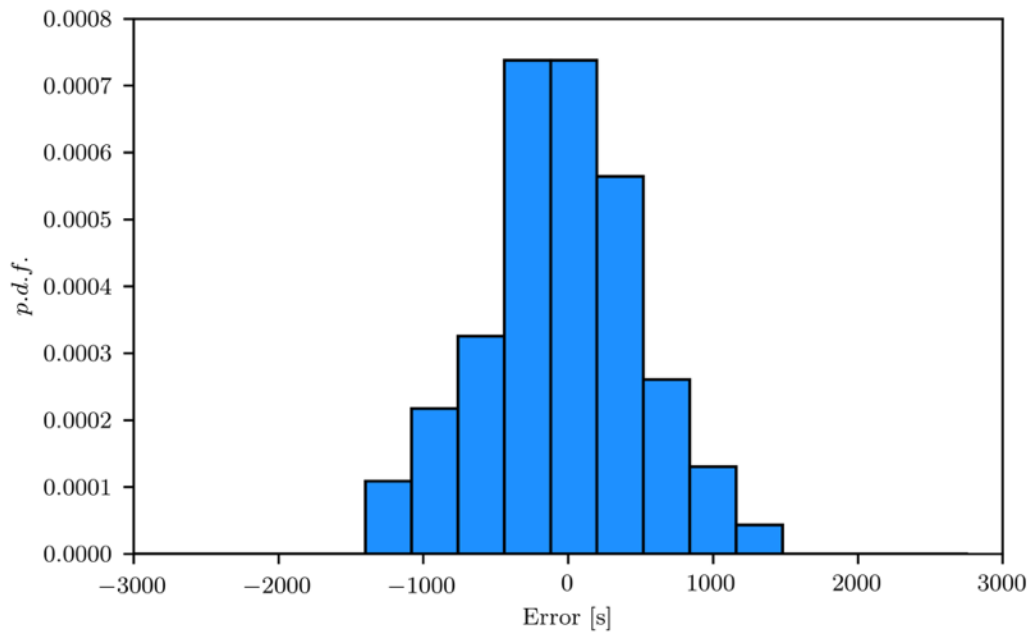
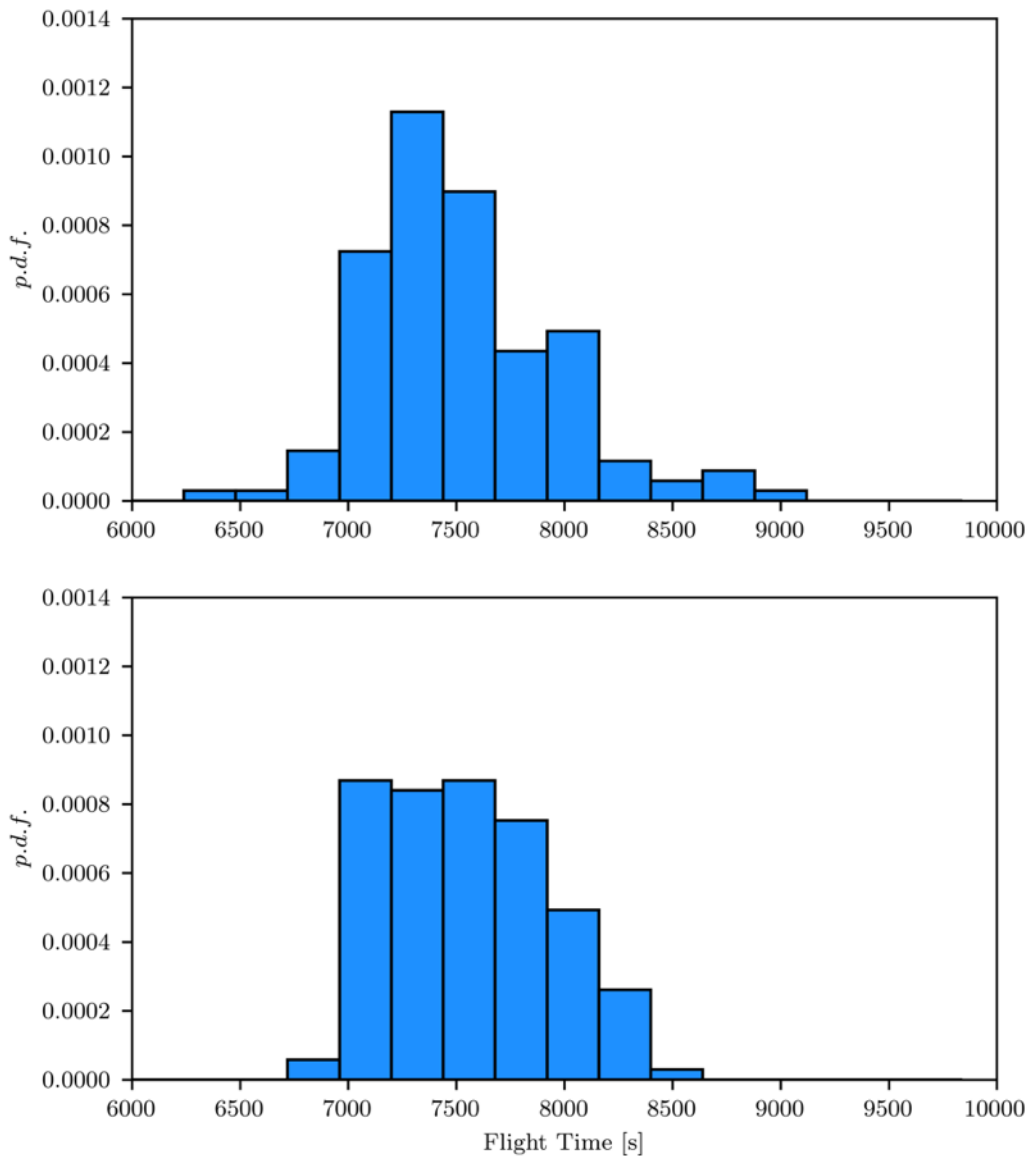


Figure 9 Probability density function of the error incurred in the flight time estimation for all flights between LEMD and EDDM during June 2018

Founding Members





**Figure 10** Probability density function of the estimated flight times for all flights between LEMD and EDDM during June 2018 by (top) the trajectory prediction tool and (bottom) the aPCE polynomials

In any case, it is observed that the aPCE methodology approximates quite well the results obtained by a complex trajectory prediction tool with a much simpler approach, and with the added benefit of taking significantly less time. For the proposed case study of 202 trajectories in which three different values are proposed for the eight aircraft intent variables, the aPCE methodology just took 37 seconds in order to compute all the proposed variations and obtain the flight time estimations, while the trajectory prediction tool required one second per computed trajectory, leading to a total of around 600 seconds required to compute all variations. This serves to show the benefits of employing the developed methodology, especially when extrapolating the case study to a large-scale scenario of thousands of trajectories which increased spectrums of possible perturbations.



#### 4.1.1 Reducing the number of uncertain aircraft intent variables

To evaluate the robustness of the developed methodology, a study case was proposed in order to check how the accuracy in the aircraft trajectory variable estimation is affected by a reduction of the number of uncertain aircraft intent variables taken into consideration. For example, in the work that served as a basis upon which the presented methodology was built [10], the aircraft intent variables considered as uncertain were only three: the Mach and pressure altitude during the cruise phase and the calculated distance to the TOD. Therefore, it is interesting to assess what would be the implications of considering a reduced set of uncertain input variables.

When selecting this reduced set, a straightforward decision is to try to reduce complexity in the parametric space defined by the perturbations of the eight aircraft intent variables considered in the first place. As it was mentioned before, some of the considered perturbations on some of the input variables led the aPCE polynomials to provide flawed results. Therefore, it is reasonable to remove those variables and keep the ones which provide robustness to the developed methodology even when heavily perturbed. As such, the same study case will be implemented again but just considering the following four uncertain aircraft intent variables:

- Mach number at climb phase
- CAS at climb phase
- Pressure altitude at cruise phase
- TOC altitude

The ones removed are those related to the descent phase, as well as the Mach number in the cruise phase. These are the ones that present more problems in the uncertainty quantification process due to the complexity in their exact determination (most times there is not a clear boundary between the cruise phase, the TOD and the descent phase), and consequently are those, as shown in **¡Error! No se encuentra el origen de la referencia.**, which present a more complex uncertainty profile. The selected aircraft intent variables to keep in the loop are those for which the full spectrum of uncertainty, as defined in **¡Error! No se encuentra el origen de la referencia.**, can be considered without leading to defective results from the aPCE polynomials.

The results obtained for the proposed case study can be observed in **¡Error! No se encuentra el origen de la referencia.** and **¡Error! No se encuentra el origen de la referencia.**. The immediate conclusion that can be extracted is that, as it could have been expected, the lower definition in the consideration of uncertainty for the proposed trajectories lead to less accurate estimations when compared to real trajectories. This is evident in the results shown in **¡Error! No se encuentra el origen de la referencia.**, where the dispersion of the incurred error is significantly higher than the one obtained with the full set of aircraft intent variables as seen in **¡Error! No se encuentra el origen de la referencia.**.

Additionally, it is seen that the flight time estimations provided with this reduced set in the aPCE polynomials are significantly worse than the ones that can be retrieved from the trajectory prediction tool, with very dissimilar distributions as depicted in **¡Error! No se encuentra el origen de la referencia.**. This leads to a reduced applicability of the developed method, as although it would reduce the computational time incurred to obtain these estimations (only 4 seconds are required to compute all variations for the 202 trajectories), it does not maintain an acceptable level of accuracy in comparison with a more traditional method such as a kinematic trajectory prediction.

Therefore, these results confirm that the application of the developed methodology requires the consideration of aircraft intent variables that covers most if not all of the phases of the aircraft trajectory, as with the reduced set, the accuracy is significantly impacted. The benefits of limiting the set of considered input aircraft intent variables come from an important reduction in the computational time, as well as a higher success rate in the issuance of flight time estimations with perturbations in all variables thanks to the reduction in complexity.

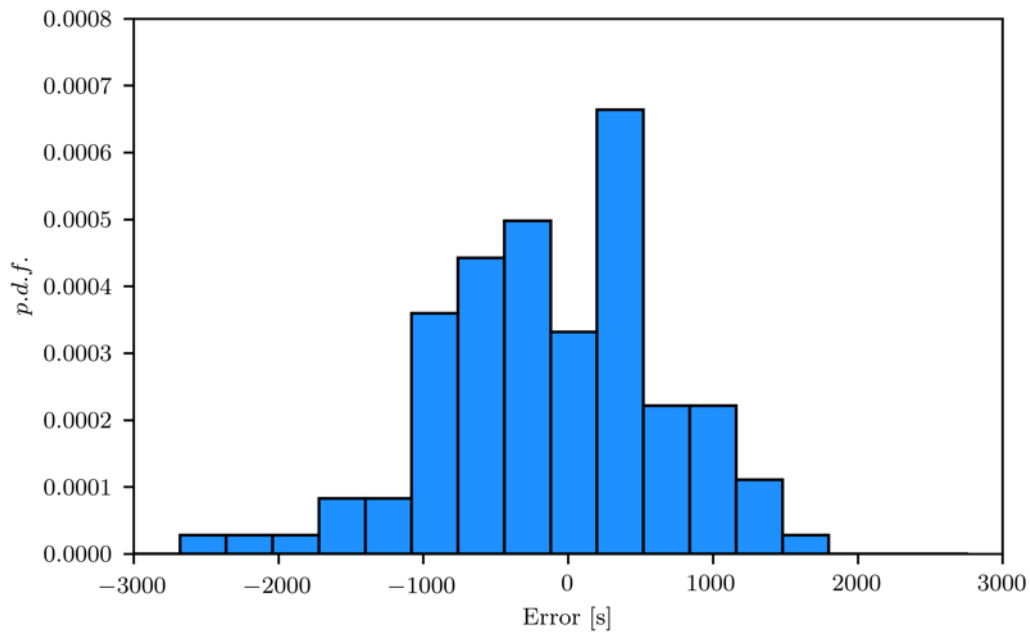


**Figure 11** Probability density function of the error incurred in the flight time estimation with the reduced set of input variables

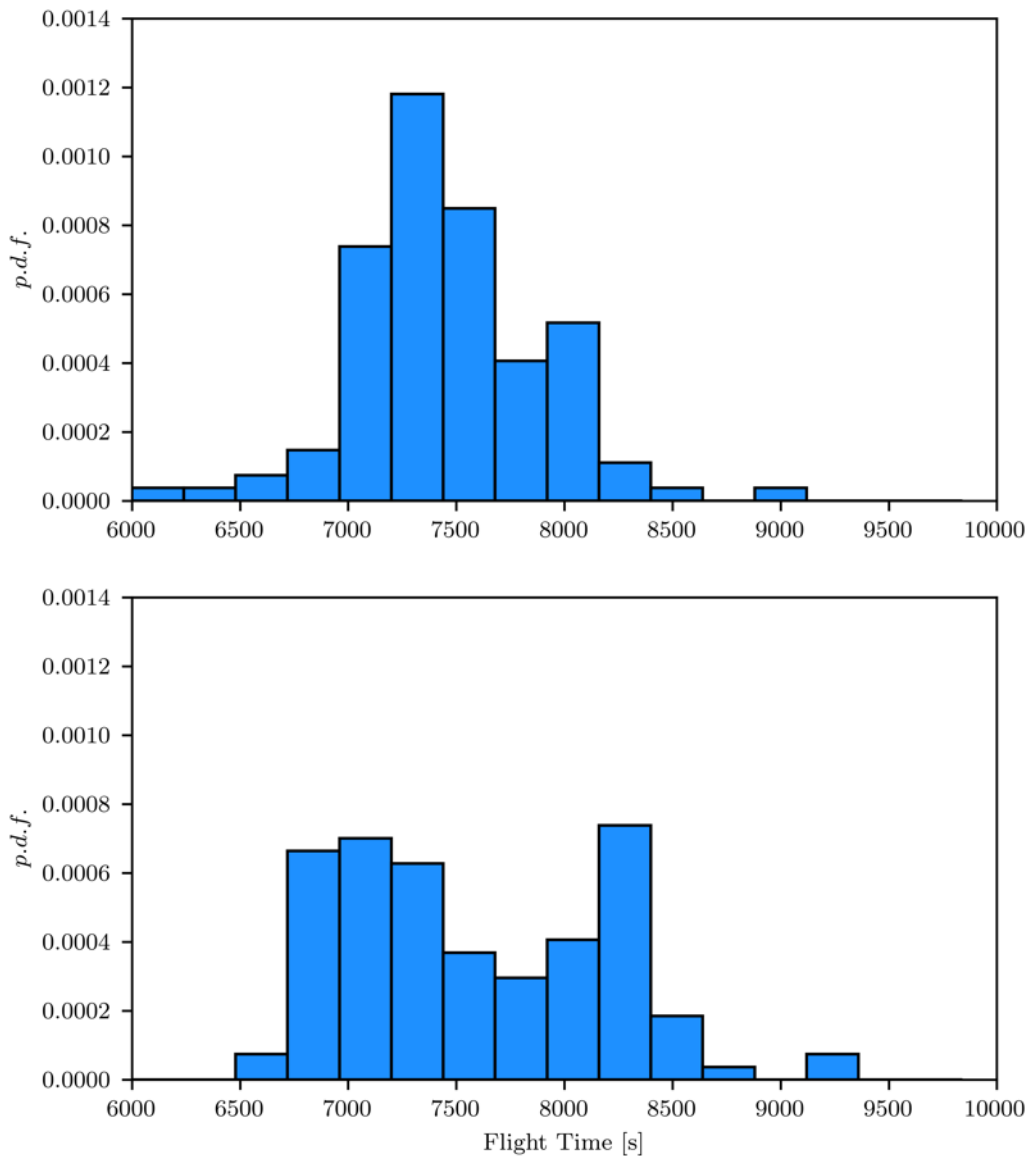


Figure 12 Probability density function of the estimated flight times with the reduced set of input variables for all flights between LEMD and EDDM during June 2018 by a) the trajectory prediction tool and b) the aPCE polynomials

## 4.2 Including uncertainty in weather conditions

Whereas the previous cases have been evaluated without taking into account the weather information, it is clear that weather plays a key role in the trajectory evolution of any flight. To include weather information into the aPCE polynomials as a few input variables, two different compressing methodologies have been evaluated: POD and CNN-AE. Both approaches have been implemented with the goal of encoding three-dimensional fields of temperature and wind velocity components into 3 latent variables.

Figure 13 shows the low-order reconstruction provided by POD approach. A visual inspection makes it clear that the large-scale structures populating atmospheric flows are well captured by the reconstructions. In the case of Figure 13, a significant large-scale structure is observed. It represents a counter-clockwise-rotating vorticity region located over the South of France, with an associated area of high temperatures. However, the predictions show attenuated values of these temperatures close to the peak. This result is expected since the truncation of POD modes is removing energy from the reconstruction. Furthermore, the vertical-velocity wind component of the predictions is attenuated with respect to its reference. This behaviour could be ascribed to the fact that this quantity does not represent a significant part of the energy content compressed by the POD, thus being represented in the largest POD modes not included in the reconstruction.

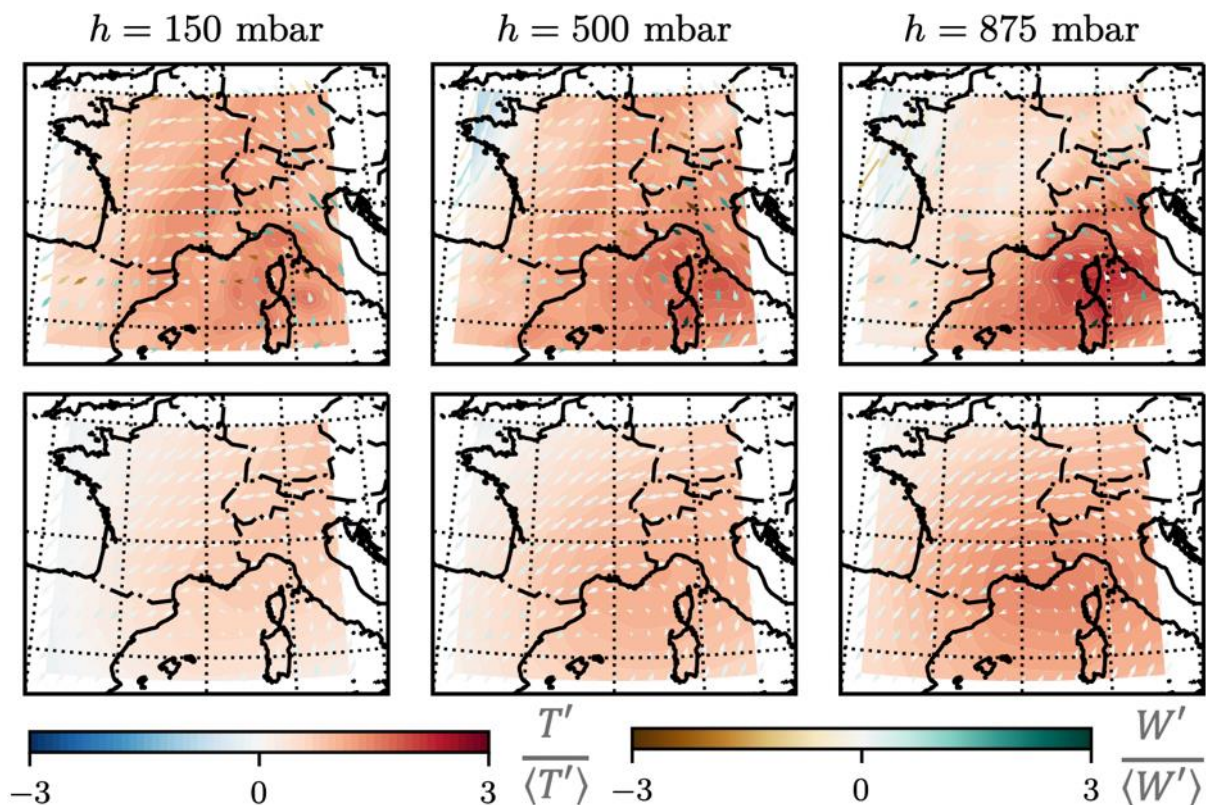


Figure 13 Results for low-order reconstruction of weather data at three different pressure levels for the POD method. Top row refers to reference data, while bottom one refers to POD low-order reconstructions. Contour plot refers to temperature fluctuations with respect to the mean temperature at each level, while arrows heading and length refer to the direction and intensity of the wind component in the Earth-surface-parallel directions. Arrow colour denotes the magnitude of the wind in the Earth-surface-normal direction. All quantities are scaled with their corresponding standard deviation.

Figure 14 shows the results for the CNN-AE compression. As in the case of POD results, it can be observed that the large-scale structures governing the atmospheric flow are well captured in the low-order reconstruction. In the same manner, the predictions tend to attenuate the values at the areas with the highest fluctuations. However, this attenuation is not caused by the same reasons as in POD, since CNN-AE does not impose a hierarchical order in the latent space based on the energy content.

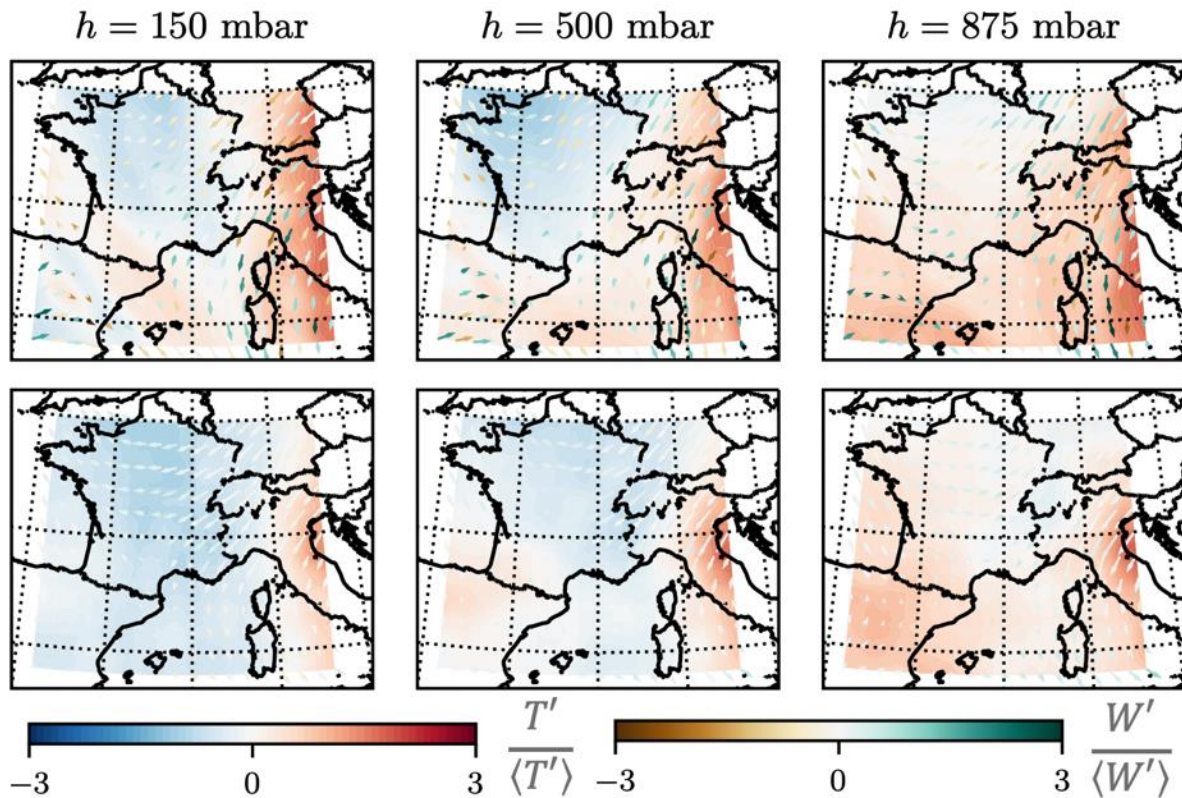


Figure 14 Results for low-order reconstruction of weather data at three different pressure levels for the CNN-AE method. Top row refers to reference data, while bottom one refers to CNN-AE low-order reconstructions. Contour plot refers to temperature fluctuations with respect to the mean temperature at each level, while arrows heading, and length refer to the direction and intensity of the wind component in the Earth-surface-parallel directions. Arrow colour denotes the magnitude of the wind in the Earth-surface-normal direction. All quantities are scaled with their corresponding standard deviation.

In order to select the most suitable method, both methodologies have been compared in terms of mean-squared error of the low-order reconstructions. Results show that the lowest overall error is reported by POD, while the different architectures tested in the case of CNN-AE are not able to improve this error. Because of this, and since POD is significantly cheaper from a computational-cost point of view, POD has been selected as the encoding methodology for this study case. In any case, the results provided here do not imply that in general POD works better than CNN-AE, but with the available amount of training data it is more suitable. This statement relies on that, during CNN-AE training, an overfitting behaviour was observed, i.e., the network was not able to generalize enough due to not high enough amount of training data.

A dataset containing the first three POD coefficients for the flights between May 2017 and May 2018 have been included to the original dataset of aircraft intent variables, thus increasing the number of dependent variables in the aPCE polynomials up to 11. In this study case however, the perturbations for the weather conditions were not considered using the EPS datasets proposed in the methodology as per Section 3.2.1.1 due to the simpler scope proposed. Instead, the reference reconstruction of weather conditions coming from ECMWF’s ERA 5 datasets will be used, considering only the potential perturbations along the flight development, that is, considering the forecast at the different issuance times in which the flight will develop (i.e., if flight is estimated to depart at 9AM, consider the

reconstruction weather dataset for 9AM, 10AM and 11AM). This constitutes a shortcoming from the process proposed by the methodology described in Section 3, as the output would be richer when considering 50 possible perturbations in the weather conditions. Then, the results to be presented are assumed to be less robust than they could be when using EPS datasets.

Figure 15 shows the error distribution for the aPCE predictions with respect to the real flight times including the perturbations for the weather uncertainty. Similar to the previous examples, the error is centred in zero. In this case, the dispersion of the error is narrower than in the reduced set of variables case, and similar to the results provided for the nominal case. Nonetheless, there are a few cases in the left side of the graph not observed in the reference case. These errors could be ascribed to the inherent complexity of including a high-dimensionality weather system into an aPCE expansion with only a few variables.

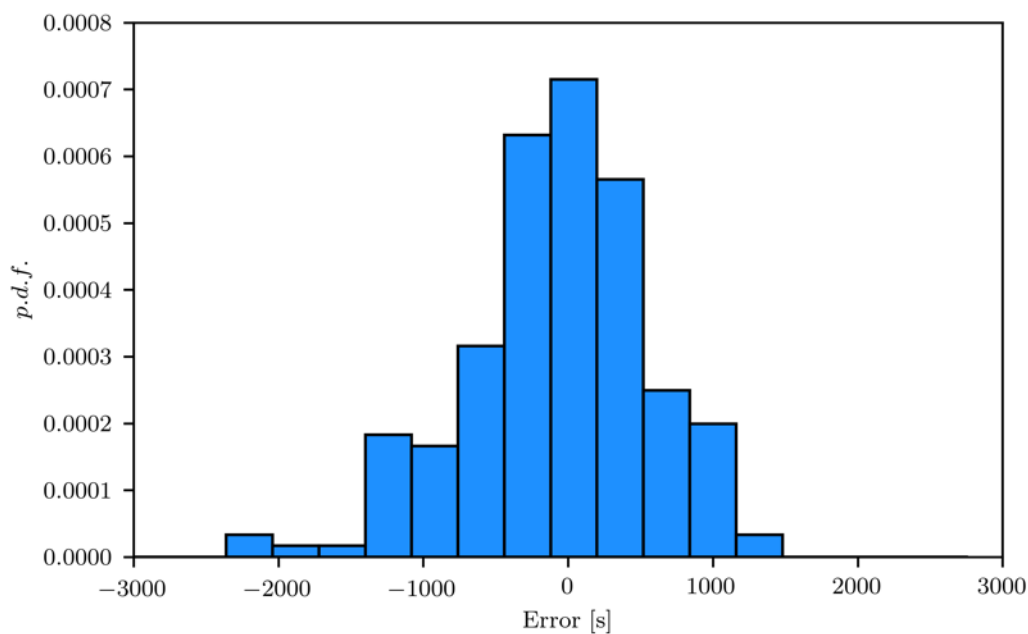


**Figure 15** Probability density function of the error incurred in the flight time estimation with the aircraft intent set of input variables together with weather variables.

Figure 16 reports the comparison between the flight times obtained from the aPCE and the real ones. As it can be observed, in this case the resemblance between the prediction and the reference is the largest one. Specifically, it can be observed that aPCE is able to cover the prediction spectrum even in the most extreme cases, i.e., in the edges of the distribution function.

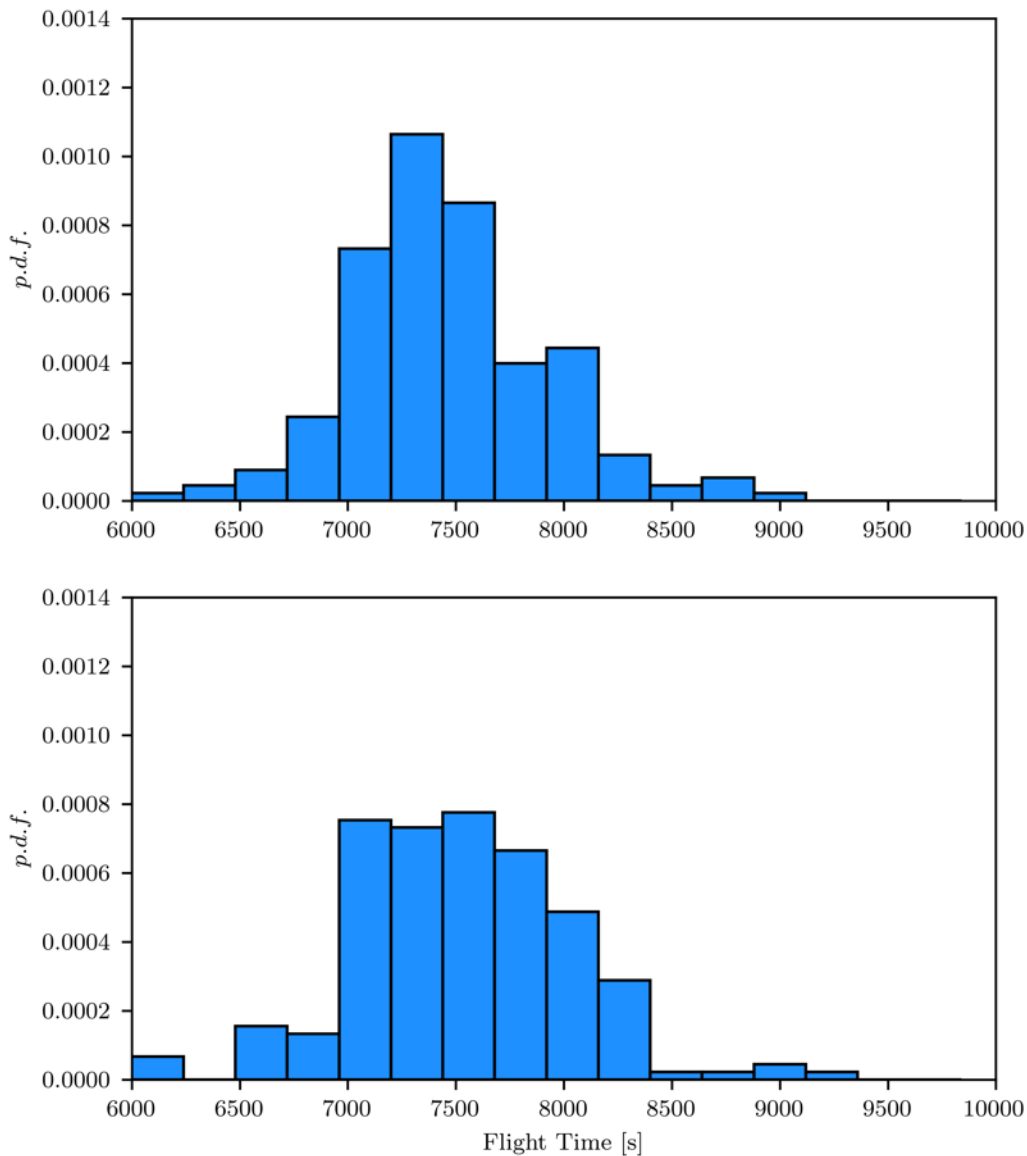


Figure 16 Probability density function of the estimated flight times with the aircraft intent and weather set of input variables for all flights between LEMD and EDDM during June 2018 by a) the trajectory prediction tool and b) the aPCE polynomials

### 4.3 Including uncertainty in initial conditions

The potential variations of the initial conditions on the development of the aircraft trajectory were identified in [2] as a source of uncertainty that should be taken into account when issuing a trajectory prediction. These conditions were mainly defined as the initial 4D position of the aircraft when starting its journey, as well as the initial mass of the aircraft.

With respect to the mass, the problem of lacking actual performance data was already identified as the main issue impeding its inclusion, since without real performance data including the mass, it is not

possible to execute the required uncertainty quantification. With respect to the initial 4D position of the aircraft, each component should be analyzed separately.

The uncertainty for the initial altitude of the flight will be considered as negligible. Once the airport of departure is well known, the initial altitude of the aircraft will be taken as the one for the reference point of the airport, as the difference between this altitude and the one for the runways can be neglected.

On the other hand, the uncertainty on the initial latitude and longitude should definitely be considered, because the departure runway configuration for any flight will significantly influence the trajectory to be described by the aircraft to the destination airport. For this purpose, a runway configuration estimation model was included within the deployed data assimilation models in order to determine which runway is to be used by the flight associated to each incoming flight plan. These estimations were executed for the proposed case study, but the estimations for the flight time were not updated including the computed initial position. This is because no significant differences in the estimated flight time were found for this case when considering the estimation for the runway configuration. If the study case were to be expanded in order to also be able to estimate other relevant aircraft trajectory parameters, such as the lateral or the vertical profile, the consideration of the estimations provided by the built runway configuration model would be much more important.

Finally, the last component of the initial 4D position of the aircraft trajectory is the initial or take-off time, for which its uncertainty should also be considered. For this purpose, the three different data assimilation models described in Section 3.2.2 are employed in order to come up with an approximated estimation of what the take-off time is expected to be for any incoming flight plan for which an estimation of the flight time needs to be issued. This approximation is built by assuming that the deviations on the initial time of the flight will be taken as the sum of the deviations on the off-block time and on the taxi time to be incurred by the operation. Therefore, when taking as baseline the time at which a given tail parks at the airport, the estimated turnaround time could be used to calculate the estimated off-block time for the next operation to be executed for the same tail, and adding the estimated taxi time, the approximated take-off time for the operation of interest can be obtained.

This approach has a shortcoming for all those flights that are served by aircraft that is already on the airport and have not executed another operation just before (e.g., early morning flights served by aircraft that arrived the night before). In these cases, the turnaround time does not serve as a good estimation of the off-block time. However, for these cases, the deviation in the initial flight time can be approximated to just that one of the taxi time, thus taking as valid the off-block time information provided in the flight plan.

Consequently, for all those aircraft that are executing consecutive operations, the process starts by identifying the arrival time at the airport of departure for the next flight, which can be gathered from the surveillance information. Then, an estimation is done by the corresponding data assimilation model on the turnaround time that will be required by the aircraft so that the next operation is started. This turnaround time is then defined as the time that the aircraft spends parked at the airport between consecutive operations. Figure 17 shows the distribution of turnaround times for E195 and A320 aircraft within the proposed study case, i.e., operating the city pair LEMD-EDDM during June 2018. This estimation, driven by the aircraft type of interest, together with the arrival time for the previous operation, provides with an estimation of the off-block time for the operation of interest. This estimation serves as an update to the planned off-block time provided within the flight plan.



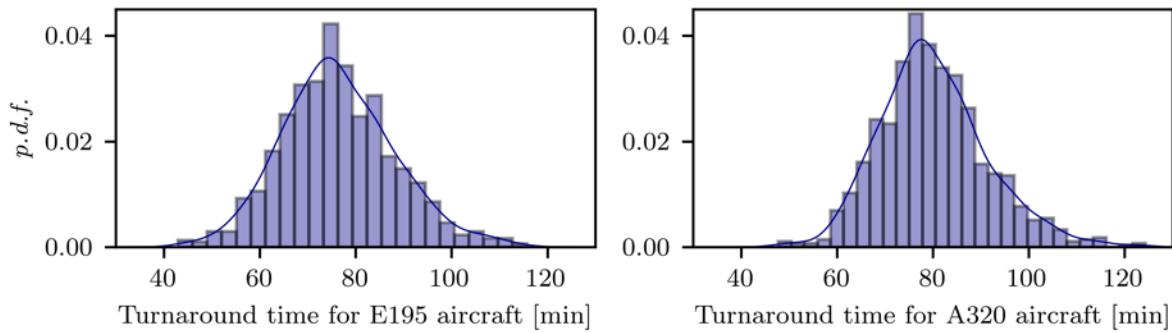


Figure 17 Probability density function of the estimated turnaround time for (left) E195 and (right) A320 aircraft operating flights with departure from LEMD to EDDM during June 2018

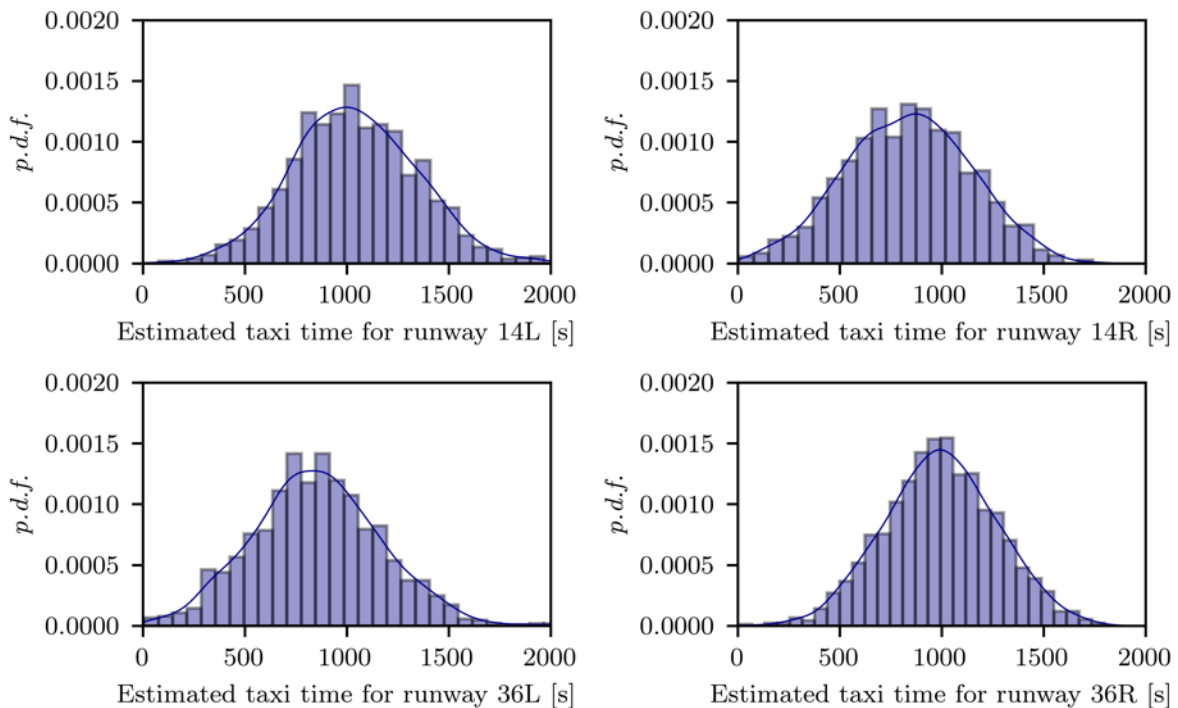


Figure 18 Probability density function of the estimated taxi times for all flights departing from LEMD during June 2018 for runway (top left) 14L (top right) 14R (bottom left) 36L (bottom right) 36R

To complement this off-block time estimation, the taxi time to be expected for the operation of interest can be issued. Using the output from the runway configuration model, a prediction of the runway to be used by the operation can be known. Then, the taxi time prediction model can provide with an estimation of the required time for the aircraft to complete the taxiing phase to the expected runway. This issued time, when added to the previously issued off-block time, results in an acceptable estimation of the take-off time for the operation of interest.

Figure 18 serves to illustrate the estimations that have been issued for the proposed case study. It presents the probability distributions for the estimated taxi time to be spent depending on the runway selected for the departure. Thus, the runway configuration estimation is the one that allows to know which runway is chosen, and thus determines the associated taxi time.



It could be argued that using these estimates could reduce the uncertainty but introduce some prediction error, as obviously the estimations provided by these models are not perfect. Although a thorough review was done on the accuracy of these estimations for the airport used in this study case, it would remain as a future work to check the increase or decrease in the accuracy of trajectory determination as a consequence of the consideration of an estimate for the initial time and location of the flight.

## 5 Concluding remarks

---

Within this document, a fully developed framework was presented in order to propagate the identified uncertainty factors affecting the trajectory in the micro-level. This framework takes into consideration the sources of uncertainty coming from the deviations in the aircraft intent and initial conditions, as well as the potential changes in the weather conditions.

The proposed methodology employs a time-dependent formulation of the Polynomial Chaos theory, that serves as an alternative to traditional methods based on Monte Carlo simulations using kinematic aircraft trajectory predictions. This formulation is complemented with a novel encoding methodology capable of compressing standard weather datasets to a few latent variables that are introduced as a necessary input within the aPCE polynomials, which allows the proposed framework to consider potential deviations in the weather conditions as posed in the perturbed weather forecasts. This is a significant improvement with respect to similar methodologies seen in the literature [10][11][12]. Additionally, a further advancement is executed by including the output of data assimilation models within the framework for determining the initial conditions to be expected for any given flight, providing estimations for factors directly influencing the initial time and/or position of the aircraft for the computation process.

The proposed study case explores the applicability and suitability of the posed methodology for uncertainty propagation in the aircraft trajectory prediction process. It shows how, when applying the framework to a relevant scenario within the European air traffic, the results obtained for estimating the probability distribution of the flight times resembles the actual values observed in reality, even when considering weather uncertainties. It obtains results comparable to those retrieved by using a complex aircraft trajectory prediction tool [27] while reducing the involved computational time and complexity, as it avoids the application of computationally demanding methods (e.g., a Monte Carlo simulation).

This use case could be expanded and improved in future iterations within the START projects. First, the reduction of uncertainty when considering estimations for initial conditions using the data assimilation models output should be assessed in a similarly relevant scenario. In this document, the approach to the inclusion of such estimations was only theoretical, so the introduction of error coming from inaccurate estimations could not be evaluated. Also, the employment of EPS forecasts for the consideration of weather perturbations was proposed within the theoretical posing of the methodology, but in the study case ERA5 reanalysis datasets were employed. The latter should be considered in an expanded use case, as it is expected to enhance the results, making the resulting probability distributions more resilient to potential deviations. Uncertainties affecting the trajectory coming from aircraft performance deviations were not considered due to the lack of required data, so further iterations should aim to include them. Finally, the only trajectory variable analyzed within the use case was the total flight time, but other relevant variables should be introduced in further iterations, such as the incurred latitude, longitude and altitude. This would allow to evaluate the time-dependence of the retrieved aPCE polynomials, as it would be possible to retrieve the probability distributions for the values of those variables in the different discrete points defined within the trajectory, and not only at the end point.

## 6 References

---

- [1] Soler, M. (2020). Project Management Plan. START Project. D1.1.
- [2] SESAR Exploratory Research (2021). Data assimilation modelling and trajectory-level uncertainty characterization. START project, D2.1.
- [3] Gerretsen, A. & Swierstra, S. (2003). Sensitivity of aircraft performance to variability of input data. EUROCONTROL, DIS/ATD Unit, DOC. CoE-TP-02005.
- [4] Bayraktutar, I. (2005). Impact of Factors, Conditions and Metrics on Trajectory Prediction accuracy. 6<sup>th</sup> USA/Europe ATM R&D Seminar.
- [5] Zeh, T., Rosenow, J., Alligier, R. & Fricke, H. (2020). Prediction of the propagation of trajectory uncertainty for climbing aircraft. In Proceedings of the 39<sup>th</sup> AIAA/IEEE Digital Avionics Systems Conference (DASC).
- [6] Zeh, T., Rosenow, J. & Fricke, H. (2019). Interdependent uncertainty handling in trajectory prediction. Aerospace 6(2), 15.
- [7] Crisostomi, E., Lecchini-Visintini, A. & Maciejowski, J. (2008). Combining Monte Carlo and worst-case methods for trajectory prediction in air traffic control: a case study. Journal of Guidance, Control and Dynamics, submitted.
- [8] Lympelopoulos, L. & Lygeros, J. (2010). Sequential Monte Carlo methods for multi-aircraft trajectory prediction in air traffic management. Journal of Adaptive Control and Signal Processing, 24(10), 830-849.
- [9] Casado, E. (2016). Trajectory prediction uncertainty modelling for Air Traffic Management. PhD Thesis, University of Glasgow.
- [10] SESAR Exploratory Research (2018). Final Project Results Report. D5.1 COPTRA, H2020-SESAR-2015-1.
- [11] Casado, E., La Civita, M., Vilaplana, M. & McGookin, E. W. (2017). Quantification of aircraft trajectory prediction uncertainty using polynomial chaos expansions. In Proceedings of the 36<sup>th</sup> IEEE/AIAA Digital Avionics Systems Conference (DASC).
- [12] Casado, E., La Civita, M., Uzun, M. Koyuncu, E. & Inalhan, G. (2018). Estimated Time of Arrival Sensitivity to Aircraft Intent Uncertainty. 15th IFAC Symposium on Control in Transportation Systems, 51(9), 162-167.
- [13] Vázquez, R. & Rivas, D. (2013). Propagation of Initial Mass Uncertainty in Aircraft Cruise Flight. Journal of Guidance, Control and Dynamics, 36(2), 415-429.
- [14] Wiener, N. (1938). The homogeneous chaos. American Journal of Mathematics, 60(4), 897-936.
- [15] Oladyshkin, S., & Nowak, W. (2012). Data-driven uncertainty quantification using the arbitrary polynomial chaos expansion. Reliability Engineering & System Safety, 106, 179-190.

- [16] Ghanem, R., & Spanos, P. D. (1993). A stochastic Galerkin expansion for nonlinear random vibration analysis. *Probabilistic Engineering Mechanics*, 8(3-4), 255-264.
- [17] Li, H., & Zhang, D. (2007). Probabilistic collocation method for flow in porous media: Comparisons with other stochastic methods. *Water Resources Research*, 43(9).
- [18] Webster, M. D., Tatang, M. A., & McRae, G. J. (1996). Application of the probabilistic collocation method for an uncertainty analysis of a simple ocean model.
- [19] Crestaux, T., Le Maitre, O., & Martinez, J. M. (2009). Polynomial chaos expansion for sensitivity analysis. *Reliability Engineering & System Safety*, 94(7), 1161-1172.
- [20] González-Arribas, D., Soler, M., & Sanjurjo-Rivo, M. (2018). Robust aircraft trajectory planning under wind uncertainty using optimal control. *Journal of Guidance, Control, and Dynamics*, 41(3), 673-688.
- [21] Sirovich, L. (1987). Turbulence and the dynamics of coherent structures. I. Coherent structures. *Quarterly of applied mathematics*, 45(3), 561-571.
- [22] Hinton, G. E., & Salakhutdinov, R. R. (2006). Reducing the dimensionality of data with neural networks. *science*, 313(5786), 504-507.
- [23] Baldi, P., & Hornik, K. (1989). Neural networks and principal component analysis: Learning from examples without local minima. *Neural networks*, 2(1), 53-58.
- [24] Goodfellow, I., Bengio, Y., Courville, A., & Bengio, Y. (2016). *Deep learning* (Vol. 1, No. 2). Cambridge: MIT press.
- [25] Nair, V., & Hinton, G. E. (2010, June). Rectified linear units improve restricted boltzmann machines. In *Proceedings of the 27th International Conference on International Conference on Machine Learning* (pp. 807-814).
- [26] Kingma, D. P., & Ba, J. (2014). Adam: A method for stochastic optimization. *arXiv preprint arXiv:1412.6980*.
- [27] Dalmau, R., Melgosa, M., Vilardaga, S., & Prats, X. (2018). A fast and flexible aircraft trajectory predictor and optimiser for ATM research applications. *Proceedings of the 8th International Congress on Research in Air Transportation (ICRAT)*. Castelldefels, Catalonia: Eurocontrol and FAA.
- [28] Soler, M. (2020). Data Management Plan. START Project. D1.2.
- [29] EUROCONTROL. (2016). User Manual for the Base of Aircraft Data (BADA) Revision 4.20. EEC Technical/Scientific Report No. 12/11/22-58.



Participant No	Participant organisation name	Country
1 - BDG	 Boeing Research and Technology Germany (BRTE)	Germany
2 - DLR	 German Aerospace Center (DLR)	Germany
3- ENAC	 Ecole Nationale de l'Aviation Civile (ENAC)	France
4- FK	<b>FL/GHTKEYS</b> FlightKeys (FK)	Austria
5- ITU	 Istanbul Teknik Universitesi (ITU)	Turkey
6 – UC3M (Coordinator)	 Universidad Carlos III de Madrid (UC3M)	<b>Spain</b>
7 - UPC	 Universitat Politècnica de Catalunya (UPC)	Spain